KR0000218
KAERI/AR-534/99

증기폭발 연구현황 보고서

Steam Explosion Studies Review

1999. 3.

한 국 원 자 력 연 구 소

Korea Atomic Energy Research Institute

Please be aware that all of the Missing Pages in this document were originally blank pages

제 출 문

한국원자력연구소장 귀하

본 보고서를 1998 년도 "격납건물 건성성 평가기술개발" 과제의 기술현황분석보고서로 제출합니다.

제목: 증기폭발 연구현황 보고서

Steam Explosion Studies Review

1999 년 3 월

주저자: 황문규

공저자: 김희동

요 약 문

냉각수가 고온의 용융물과 접할 때 이 용융물의 미세한 분쇄와 이에 따른 냉각수로의 급격한 열전달로 인해 수증기가 폭발적으로 발생할 수 있는데 이 현상을 증기폭발이라 부른다.

증기폭발 현상에서 이에 참여하는 용융물이 많을 경우에는 이로 인한 기계적 에너지의 부하는 상당량에 달해 주변 구조물에 건전성을 위해할 수 있는 충분한 상황이 된다. 따라서 원자로의 노심용융물 동반한 중대사고 시 고온의 노심 용융물은 냉각수와의 접촉으로 증기폭발을 일으킬 수 있게 되고, 이 현상으로 인해 궁극적으로 격납건물의 건전성을 상실할 가능성도 있다.

그간 증기폭발현상을 이해하려는 노력으로 상당한 연구가 진행되어 왔다. 본 보고서에는 이 증기폭발 현상에 대한 실험적 그리고 이론적 연구를 정리한다. 실험적 연구의 경우 보통 20g 이하 질량의 용융물을 다루는 소형실험과 1kg 이상을 용융물로 쓰는 중대형 실험을 모두 다룬다. 또, 이론적 연구에 대해서는 열역학적 모델 및 현상의 진행과정도 포함시키는 기계적 모델도 정리한다.

Summary

When a cold liquid is brought into contact with a molten material with a temperature significantly higher than the liquid boiling point, an explosive interaction due to sudden fragmentation of the melt and rapid evaporation of the liquid may take place. This phenomenon is referred to as a steam explosion or vapor explosion.

Depending upon the amount of the melt and the liquid involved, the mechanical energy released during a vapor explosion can be large enough to cause serious destruction. In hypothetical severe accidents which involve fuel melt down, subsequent interactions between the molten fuel and coolant may cause steam explosion. This process has been studied by many investigators in an effort to assess the likelihood of containment failure which leads to large scale release of radioactive materials to the environment.

In an effort to understand the phenomenology of steam explosion, extensive studies has been performed so far. This report presents both experimental and analytical studies on steam explosions. As for the experimental studies, both small scale tests which involve usually less than 20g of high temperature melt and medium/large scale tests where more than 1 kg of melt is used are reviewed. For the modelling part of steam explosions, mechanistic modelling as well as thermodynamic modelling is reviewed.

TABLE OF CONTENTS

LIST OF FIGURES

1. Introduction

When a cold liquid is brought into contact with a molten material with a temperature significantly higher than the liquid boiling point, an explosive interaction due to sudden fragmentation of the melt and rapid evaporation of the liquid may take place. This phenomenon is referred to as a steam explosion or vapor explosion.

Large-scale vapor explosions initiating from melt-on-coolant contact are known to go through four distinct phases; namely, coarse mixing, triggering, propagation, and expansion. As the hot melt falls into the liquid coolant, it breaks up into globules nearly 1cm in diameter in the case of molten corium and water. Film boiling occurs at the surface of each hot globule without significant heat transfer from the melt to the liquid coolant. In this phase, the melt drops, vapor film, vapor bubbles, and liquid coolant remain in a metastable condition. The process called premixing can last about one second. The metastable stage of coarse mixing can be transformed to liquid-liquid contact between the melt and coolant by disturbance of the vapor blanket around the melt. The process can happen spontaneously, usually next to solid surfaces in a confined geometry, or can be initiated by a pressure pulse which locally destabilizes the film layer between the melt and coolant. This triggering phase initiates efficient heat transfer between the liquid coolant and the molten material. Following the triggering phase, high pressure coolant vapor is generated, and a disturbance pulse travels through the whole coarse mixing region leading to direct contact between the molten material and liquid coolant. In this stage named propagation phase, part of the molten liquid undergoes fine fragmentation resulting in very large melt-coolant interfacial area, which in turn leads to higher heat transfer between the two. Finally, the high pressure vapor generated in the propagation

phase expands against the surrounding material. Part of the thermal energy transferred from the molten material to the coolant is transformed into mechanical energy during this phase, and may result in the destruction of the surrounding structures. This phase is called expansion.

Steam explosions have been of concern in the nuclear industry. In hypothetical severe accidents which involve fuel melt down, subsequent interactions between the molten fuel and coolant may cause steam explosion. This process has been studied by many investigators in an effort to assess the likelihood of containment failure which leads to large scale release of radioactive materials to the environment.

In this report, earlier work on steam explosions is reviewed. Chapter 2 summarizes the results of earlier experimental studies; both small and intermediate/large scale experiments are reviewed. Theoretical models of vapor explosions are summarized in Chapter 3.

2. Experimental Studies

Experimental studies of vapor explosions are usually classified into two categories, namely, small scale and intermediate/large scale. The difference depends on the amount of fuel and coolant liquid involved in the interactions. Small scale experiments which usually involve less than 20 grams of melt may not precisely represent the real propagating event and the resulting destructive phenomena. These Intermediate or large scale experiments, on the other hand, involve more than 1 kg (up to ≈20kg) of melt. More than one unit cell is involved in such experiments. The main purpose for this type of experiments is to provide an integrated picture of all experiments, however, have been useful for the investigation of some of the basic processes which take place during vapor explosions, such as fuel fragmentation and pressure pulse behavior. They are generally preferred due to their relatively simple and safe setups which makes them accessible as laboratory level studies. Experimental observations indicate, however, that small scale experiments represent a unit cell of the more realistic large scale interaction. This generally preferred due to their generally preferred due to their generally preferred due to their means that the propagation phase of the explosion cannot be observed in such small scale experiments.

Intermediate or large scale experiments, on the other hand, involve more than 1 kg (up to ≈20kg) of melt. More than one unit cell is involved in such experiments. The main purpose for this type of experiments is to provide an integrated picture of all phases of the explosion, as well as investigating the initial conditions for triggering and propagation, quantifying the magnitude and time characteristics of the pressure pulses, and mechanical work produced.

The difference between small and intermediate/large scale experiments is important because a small scale test involves a single fuel drop or a few particles and spatial propagation of the interaction is not always possible. This chapter reviews both types of experiments in order to

provide an understanding of the various aspects of vapor explosion experiments. It is noted, however, that some of the experimental results are not fully understood and that many of the experimental results are not necessarily reproducible.

2.1 Small Scale Experiments

The usual set up for these experiments involves dropping a few grams of the molten material into the volatile coolant by tilting or unplugging a hole in the bottom of a furnace or a melt crucible. The drops fall a few centimeters into a container holding typically one liter of water. Some other experiments used floodable arc-melters, where melt was generated on the copper hearth by an arc electrode and eventually flooded with the coolant liquid.

In many cases, triggering was not spontaneous. External triggering methods such as mechanical shock or exploding wire immersed in the coolant were used, in such cases. Pressure transducers, and fast motion pictures were used in many of these tests to record the pressure history and the evolution of explosion zone volume.

Experimental data for low melt temperature metals have been conducted by many investigators [1-8]. Aluminum, lead, tin, and bismuth have been used in these small scale experiments. Among the observations made in these experiments are:

1) There is a dwell time between initial entry of the melt and start of the fragmentation. The effect of the melt and coolant temperatures on dwell time was investigated by Bjornard et al. [4]. It was observed that as the temperature of the molten drop was increased, the dwell time was also increased for a given water temperature (21 °C). However, they observed a slightly decreased dwell time when the water pool temperature was reduced from 40 °C to 30 °C and 20 °C with fixed molten temperature of 500 °C. Also, low frequency (about 1 kHz) pressure pulses with high amplitude("big bang") were observed to follow the dwell time during which high frequency (about 15 kHz) low

amplitude pressure pulses were recorded.

2) There was a melt temperature boundary below which no explosion was observed especially with tin and water combinations. The temperature in this case was around 300 °C regardless of water temperature. The effect was studied by Dullforce et al.[6]. The data showed that above the limiting temperature (300 °C) there is a linear relation between melt temperature and water pool temperature which determines the boundary of explosive versus non-explosive regions.

3) An increase in the viscosity of the coolant (by adding soluble materials) impedes the fragmentation process. The effect was studied by Nelson and Guay [8] at Sandia National Laboratories. The higher viscosity was believed to increase vapor layer stability, thus reducing fragmentation.

It should be noted, however, that many of the experiments were not repeatable. In most cases, the number of similar experiments conducted was not large enough to make the results statistically meaningful. In addition, for some experiments, the range of the independent variables was not wide enough to reach general conclusions.

Small scale experiments involving high melting point melt material were performed by Nelson and Buxton [9]. Experiments were conducted using stainless steel, metallic Corium-E simulant, and oxidic Corium-E simulant. The stainless steel experiments did not produce any violent explosions even when external triggering was used. Metallic Corium simulant was not easy to melt because of phase separation; again, for those experiments no explosion resulted. The oxidic Corium simulant, on the other hand, produced vigorous explosions at a few milliseconds delay after small initiating pressure transients were applied to the system. No spontaneous explosions were observed when external triggering pulses were not used.

More extensive studies have been performed by Nelson and Duda [10,11] using high

melting point materials. Molten iron oxide (T ≅1870K), which was considered a good simulant of molten nuclear reactor core materials, was used with liquid water as a coolant. CO_2 Laser was used to melt the iron oxide. A droplet diameter of 2.9 mm could be obtained using this device. Experiments were conducted at various ambient pressures, water temperatures/subcooling, and melt temperatures. The main observations derived from these experiments are:

1) Spontaneous triggering was observed with reduced drop fall height of the melt. When the fall height was above a certain distance, external triggering (exploding wire) was necessary. In this case, it was postulated that the larger air bag volume entrained as the molten fuel dropped was the cause of hindrance of spontaneous triggering by stabilizing the vapor film layer.

2) The maximum pressure was generated at melt temperatures of about 2500K, below or above which reduced pressures were recorded. The water temperature for this test was 298 K and the ambient pressure was 0.083 MPa. The external pulses were applied with peak pressure of around 0.7 MPa.

3) With more subcooled water (T_{sub}=97 K vs. 70 K) for a given ambient pressure, lower peak triggering pressures were required to initiate the explosion.

4) With higher ambient pressure, generally higher peak pressures were observed from the explosion. The relation was approximately linear. There was, however, no obvious relation between the generated pressure peak and the triggering pressure. With a constant water coolant temperature, the triggering pressure needed to initiate explosion was lower at pressures within a certain range (0.2 MPa - 0.8 MPa). Outside that range, higher triggering pressures were required. Another trend observed with higher ambient pressure was increased fineness of the debris from fragmentation.

5) When the melt viscosity was varied by varying the molten oxide composition (FeO_x, SiO_2, Al_2O_3), it appeared that the higher viscosity tends to reduce interactions.

In addition to the above observations, the shape of the debris, both from completely molten drops and partially solidified drops, was scanned using electron micrographs. Even with partially solidified drops (wall thickness was in the range of 100-200 μm), no apparent observation was made to verify debris from brittle fracture of a solid. The general shape was spheroidal.

Several studies have been performed which examined the effect of coolant viscosity on the likelihood and severity of vapor explosions. In general, viscous coolants suppress explosions [12, 8, 2]. They cause falling droplets of melt to entrain more air upon entry into the coolant (which stabilizes film boiling [8]), and they may damp oscillations in the boiling layer [12]. Several studies have reported that extremely viscous coolants suppress explosions, for example, Kim [12], Nelson and Guay [8], and Flory [2]

Kim studied triggered explosions of iron oxide in aqueous solutions of cellulose gum and determined the efficiency of explosions following applied trigger pressures of 200 and 400 kPa. For the 400 kPa case, the efficiency clearly drops from approximately 6 %to almost 0 % as the solution viscosity increased from 40 centipoise to 240 centipoise (corresponding to solution viscosity ratios from approximately 40 to 240). Nelson and Guay used aqueous solutions of glycerol and cellulose gum to increase the viscosity of the coolant. They observed that the depth at which spontaneous explosions of tin occurred increased as the solution viscosity increased. When the viscosity of the cellulose gum solutions exceeded approximately 15 centipoise the molten tin fell to the bottom without explosions. (This viscosity value was measured very near the solution boiling point; the viscosity of the solution at 25 °C was approximately 25 centipoise.) Flory et al. used carboxymethyl cellulose to increase the viscosity of water by approximately 5 times and found that the fragmentation of tin and other metals was greatly

reduced or totally prevented.

On the other hand, McCracken [13] observed more complicated behavior: viscous solutions of sugar and glycerol decreased the fraction of the tin sample which was finely fragmented due to spontaneous explosions (with respect to results in pure water) when the coolants were at 20 °C but increased the fragmentation at higher temperature. (In McCracken's experiment the weight percentage of sugar or glycerol was held constant while the solution viscosity varied with coolant temperature.) He also observed that when explosions did occur in the viscous solutions, they appeared to be more violent than those in water. Nevertheless, McCracken concluded that coolant viscosity was not an important parameter in vapor explosion phenomena. Detergent added to lower the surface tension of the coolant also had a negligible effect in his experiments.

Nelson and Duda [10,11] examined the importance of coolant composition by comparing results for pure water, pure n-pentadecane (a paraffin hydrocarbon), and an aqueous solution of ammonium sulfate. Their triggered experiments with molten iron oxide were performed with the same apparatus used by Kim [12]. The paraffin hydrocarbon was flammable, and the resulting noncondensable gas stabilized film boiling as the molten metal descended and completely prevented explosions. Ammonium sulfate, a soluble salt which has reportedly suppressed vapor explosions in a system of molten salt/water [14], did not suppress triggered explosions of the iron oxide when used in a 20 $^{w}/_{o}$ solution.

Obviously, extremely viscous solutions can suppress spontaneous explosions. Experimental data and hypothetical models of the fragmentation process indicate that several other coolant parameters should influence vapor explosions (see [15] and references therein), including boiling heat transfer properties and surface tension. The fragmentation observed during a vapor explosion is believed to be caused by the rapid expansion of coolant embedded beneath the surface of the molten metal by liquid jet [15]. The viscosities and surface tensions of the melt

and coolant (and their temperature dependence) and the coolant's ability to wet the melt surface will control mixing properties, interface properties, and the formation of jets. The coolant's boiling heat transfer characteristics will affect the heat transfer from melt to coolant.

Most recently, Dowling, Ip, and Abdel-Khalik [16] experimented with dilute solutions of four water-soluble polymers to examine their ability to suppress spontaneous vapor explosions. Two of these additives did not affect the surface tension of the coolant; the other two did not decrease it by more than 10% even at the highest concentrations examined. Their results suggested that dilute solutions of polymeric additives, particularly poly(ethylene oxide), may be used to completely suppress vapor explosions if, and only if, it can be assured that the concentration can be maintained above a threshold value. Their data indicated, however, that at lower concentrations, more violent, yet less frequent, explosions may result.

The effect of coolant surface tension on vapor explosion severity has not been studied as extensively as has coolant viscosity. Surface tension reducing surfactants have, however, in a similar context, been studied to determine their effect on liquid-vapor interface stability, and for use in applications such as quenching of molten materials [17]. Becker and Lindland indicate that surfactants have been applied with satisfactory results for several years in the metallurgical industry in Norway. In this respect, small amounts of surfactants are added to water for the production of copper and ferrous alloy granulate by the quenching of molten metals.

The idea of using surfactants to suppress vapor explosions was originally suggested by Groenveld [18] and more recently by Becker and his co-worker [17,19]. It is based on the surfactant's ability to stabilize the vapor film which surrounds the melt by forming a layer of surfactant molecules at the coolant-vapor interface. Becker [17] states that the surfactant layer at the interface tends to decrease the surface tension of the bulk liquid, increase the coolant surface viscosity, increase the coolant surface density, and impose a rigid surface on the vapor bubble. Surfactants also affect the formation of new surface (for example, as bubbles grow within the

liquid) since surfactant molecules migrate from the bulk of the liquid to the new interface at a finite rate [20].

Vapor explosion experiments involving surface tension reduction have been performed by Groenveld [18], Becker [17], Nelson et al. [21], and Kowal, et al [22]. Becker [17] reviewed measurements of bubble rise velocities and presented data for new surfactants. In general, the addition of surfactants decreases the velocity of gas bubbles. This result was attributed to the increased rigidity of the interface (hence, increased drag) due to the surfactant molecules.

Nelson et al. carried out small-scale vapor explosion experiments to study the effect of surfactants on hydrodynamic fragmentation and vapor explosions. This work was sponsored in part by the Swedish Nuclear Inspectorate, and the results of the experiments are also discussed in the sponsor's report by Becker and Lindland [17]. Both spontaneous explosions in a tin-water system and triggered explosions in a thermite-water system were performed, but the spontaneous experiments with tin are discussed only in Reference [17]. The majority of the spontaneous tin-water experiments were performed by dropping 12 grams of molten tin at 650 °C into a water/ethoxilated-nonyle-phenole solution. Although a few exceptions occurred, it was reported that the spontaneous vapor explosions were generally mitigated or completely suppressed by the addition of 1-10 wppm of the surfactants of the water. For the triggered thermite-generated melt experiments, use of aqueous surfactant coolant solution also reduced the severity of the interactions. Based on these results, Becker suggested that small amounts of surfactants be added to emergency cooling water in light water reactors under severe accident conditions.

Experiments were recently performed by Wiktor Frid of the Swedish Nuclear Power Inspectorate to examine the effect of coolant surface tension [23]. In over 80 tests, he dropped 80 mg of iron oxide, heated with a laser to approximately 2000 K, into a tank of subcooled water whose temperature ranged from 20-50 °C. Concentrations ranging 1-40 wppm of the

same surfactants used by Becker et al. [17] and Kowal et al.[22] (ethoxilated-nonyle-phenole and sodium-dodecyl-benzene sulfonate) were added to the coolant. Frid concluded that, in general, small amounts of surfactant at elevated coolant temperatures tended to reduce the ``explosivity'' of the molten droplets based upon pressure and particle size data. Explosive interactions occurred in the majority of the experiments carried out with surfactant solutions at temperatures less than 50 °C, however, and in one experiment with surfactant added to the coolant the energy conversion ratio was found to be 30 % - considerably higher than any previously measured in pure water. Due to the fact that only a few experiments were performed for each set of conditions, no meaningful statistical conclusions could be drawn.

More recently, Kowal et al. [22] conducted experiments involving surfactant solutions at concentrations of 5, 10, and 50 wppm. They dropped 12 grams of tin into aqueous solutions of surfactant solutions at room temperature. Twenty experiments were performed for each solution. The peak pressures for each experiment were recorded and statistically compared with those for deionized water. Additionally, particle size distributions of the fragmented debris were measured and statistically analyzed. On average, they concluded that the surfactants did mitigate the explosions, resulting in an average 65% reduction in the average peak pressures when compared to deionized water. The debris analysis supported this conclusion, indicating a 19% reduction in the fraction of the debris particles participating in the explosion when surfactants were present. Statistical analysis showed that the differences between the water and surfactant solutions were significant for both the peak pressure and particle size distributions. No differences between the ionic and non-ionic surfactants were shown. While none of the explosions were completely suppressed, this work provides strong support for the hypothesis that the presence of surfactants can mitigate vapor explosions.

To date, however, almost all small-scale experiments involving coolant properties have been conducted using pure water as the coolant or with solutions prepared using pure water, without considering the potential effect of other chemicals normally found in reactor cooling water.

For example, the emergency cooling water for an LWR contains high concentrations of boric acid. The effect of boric acid on the severity of the fuel-coolant interactions in a small scale tin-water system was recently examined by Skelton[24].

Another study involving the addition of boric acid to the coolant was conducted by Buxton, Nelson, and Benedict [25], who performed experiments with various LWR core material simulants by arc-melting 10-37 grams of the samples and then flooding the chamber with 1.5 liters of coolant solution. Explosions were initiated with a pressure transient from an exploding bridgewire. When boric acid was added (3000 ppm boron as H_3BO_3), explosions occurred with both iron oxide simulants tested; no major differences were observed from experiments with pure deionized water. However, because of the small number of experiments reported, no meaningful statistical conclusions can be drawn from such data.

The experiments conducted by Skelton [24] were repeated numerous times to allow for statistical comparisons between data for pure water and boric acid solutions. Additionally, the study investigated the effect boric acid might have on the ability of surfactants to mitigate vapor explosions. The surfactants selected, nonylphenol polyethylene glycol ether (a non-ionic surfactant) and dodecylbenzene sulfonate sodium salt (an ionic surfactant), were the same as those examined by Becker, et al. [17,19], Kowal, et al. [22], and Frid [23]. The results of Skelton [24] indicate that the presence of boric acid negates the potentially mitigating effects of the surfactant additives previously reported in experiments where the surfactants were added to pure water.

The above discussion clearly indicates the usefulness of the small scale experiments which have provided valuable information primarily about the fragmentation process, vapor dynamics in vapor explosions, and the effect of coolant and melt properties on the severity of the explosions. In the absence of a comprehensive theory, however, scaling laws governing vapor explosions are not clearly known and as a result it is believed that small scale experimental data

can not be extrapolated to large scale systems with confidence.

2.2 Medium/Large Scale Experiments

Among the experiments performed on large scale vapor explosions, there are several major investigations; these are reviewed below.

Winfrith Experiments

As a part of the vapor explosions program started in 1975 at AEE Winfrith, Briggs [26] conducted large scale experiments primarily to study the propagation phase of metal/water interactions. The test facility, THERMIR, was a 60 cm diameter vessel with a crucible on top of it (Figure 1). Up to 20 kg of molten aluminum at 1020-1979 K were discharged from the top of the vessel in each test. Molten tin was also used in a few tests. The falling distance of the melt was 0.5 to 1.1 m. The experimental setup is shown in Figure 1. In these experiments, explosions did not always occur for the same initial conditions. When explosions occurred, long dwell times (about 1 sec) between the initial entry of the melt into water and the triggering of the explosion were observed. The speed of the propagation front was measured to be about 200 m/sec in these experiments. However, the existence of a shock front was not clearly seen.

The work of Briggs was continued by Fry and Robinson [27] who used the same THERMIR facility. These experiments included an optional external trigger and an additional large narrow vessel 8 cm wide,45 cm deep, and 45 cm long. Up to 16 kg of molten tin or aluminum with a temperature of about 800 °C was introduced into water at atmospheric pressure over a wide range of water temperature. A number of experiments were conducted with low temperature tin to determine the effect of fuel temperature well below the spontaneous nucleation temperature for water.

During the experiment, basically three types of interactions were observed. These were: (1) a coherent interaction between large masses of melt and coolant, (2) localized interaction in

which a separate drop of metal or a small region of metal/water mixture interacts, and (3) incoherent interaction of large mass of metal/water mixture.

In the case of coherent interactions, the usual sequence of coarse mixing, a triggering event, and propagation of interaction through the coarse mixture were observed. When the interaction was incoherent, there was no clearly defined propagation front, resulting in a slow increase of pressure with a fairly large number of locations of interactions.

Coherent interaction was observed in a coarse mixture with high proportion of metal to water, whereas in more dilute mixtures of tin/water coherent interactions were not observed. Some of the results, however, showed that this type of incoherent interaction could develop into coherent propagation, and hence that it could be involved in an escalation phase.

As shown in Figure 2, the propagation velocity in tests with coherent interaction was proportional to the square root of the pressure peak, which is consistent with shock wave theory. During the tests with low temperature tin (300 °C) and low sub-cooling of the water (about 4 °C) coherent propagation was observed (3 times out of 5 tests).

Sandia Experiments

Large-scale vapor explosion experiments have been carried out at Sandia National Laboratories in two different series, namely, Open Geometry, and the Fully Instrumented Test Series (FITS). The purpose of the experiments was to measure the conversion ratio, and to identify the magnitude and time characteristics of the pressure pulses and initial conditions necessary to trigger and to propagate explosive interactions between water and molten materials possible in LWR accident scenarios.

In the open geometry tests, reported by Buxton and Benedict [28], the iron/aluminum oxide melt was poured by unplugging a discharge hole or opening a trap door at the bottom of the melt generator into an open cylindrical tank 0.9 m in diameter and 1.1 m high, which is partially

filled with water (175-840 kg) with minimal instrumentation. The main purpose of the experiment was to determine the conversion ratio of the fuel thermal energy to mechanical work during a reasonably large vapor explosion with melt quantities of 1 to 27 kg and temperature of about 3000 K. Spontaneous explosions were observed in these tests after a random time delay of the order of 1.5 second between start of pour and explosion. Multiple explosions occurred in some tests. Regardless of delay time or the triggering method, conversion ratios of about 0.2 % to a maximum of 1.34 % were recorded. Also, the use of saturated water appeared to have no effect on the conversion ratio. Generally, tests with smaller fragment mean diameters resulted in higher efficiency. Peak pressure amplitudes of 5 to 10 MPa with a few milliseconds of duration were usually obtained in these tests. When Corium-A+R were used, no energetic explosion was observed, and the conversion efficiency dropped to less than 0.05 %

The FITS experiments were performed in a large chamber equipped with devices for monitoring the explosion and collecting the resulting debris (Figure 3). The main objective of these tests was to measure the energy conversion ratio and examine its dependence on the initial and boundary conditions. The FITS experiments consisted of three separate series, as explained below. In the FITS-A series, a total of 5 tests was conducted by releasing 1.94-5.38kg of molten iron alumina into water (Mitchell et al. [29]). Spontaneous interactions occurred in the first three tests conducted at 0.083 MPa ambient pressure. In the fourth tests which was carried out at an elevated pressure of 1.02 MPa, a spontaneous explosion did not happen. However, a triggered explosion could be initiated at a similar ambient pressure (1.09 MPa) during the fifth test. In the FITS-B series reported by Mitchell and Evans [30], a large mass (about 18.7kg) of molten iron alumina was dropped into water with 1.5-15 times greater mass than that of the melt. Single and double explosions occurred with subcooled water, while a test with saturated water did not result in an explosive interaction. The energy conversion ratio was estimated to be between 0.3% to 1.6%.

In the FITS-C series reported by Evans et al. (Berman [31,32]), 11.5-19.5 kg of molten iron-

alumina or Corium A+R melts were released into water at nearly constant subcooling of about 70 °C at ambient (0.083 MPa) and elevated (0.52, 0.55 MPa) pressures. No explosions resulted with iron-alumina melt within this pressure range. One of the corium A+R tests (at ambient pressure) resulted in a double explosion qualitatively similar to typical iron alumina tests, while the other test did not results in an explosion.

The following remarks can be made based on the observations reported for intermediate/large scale vapor explosion experiments.

1) Following the initial contact between the melt and the cold liquid, there is a quiescent period or dwell time, prior to the explosion. This dwell time varies between a few milliseconds and more than one second. A vapor film separates the hot and cold liquids during this period.

2) The dwell time is ended by the "Triggering" process, when the quasi-stable configuration of vapor film separating the two liquids is disturbed, either spontaneously or by an external pressure pulse. In most cases, it is possible to artificially trigger an explosion in mixtures when triggering did not occur spontaneously.

3) In all experiments where explosive interaction and pressurization occurred, at least some of the molten material fragmented. The fragment size is typically of the order of 100 μm.

4) The vapor generation and fragmentation following direct liquid-liquid contact may propagate coherently throughout the coarsely-mixed medium. It appears that coherent propagation is necessary for energetic events with high conversion efficiency. No coherent propagation appears to results in small conversion efficiency.

5) Fragmentation and vapor production occur in a short time scale compared to the time required for the expansion of the vapor bubble in small-scale tests. Similarly, in large

scale experiments the propagation front moves with a supersonic speed and the expansion of the produced vapor during the interaction process is negligibly small.

FARO Experiments

The faro tests were designed to provide data on mixing and quenching of large masses of real corium materials in water under severe accident prototypical conditions [33,34]. Quantities of the order of 150 kg of UO_w/ZrO_2 and $UO_2/ZrO_2/Zr$ mixtures are used. Basically, the penetration of the molten corium into the water at the lower plenum and its subsequent settling on the bottom head of the RPV are simulated. So far, the knowledge in this area was based essentially on small scale mixing and separate effect tests. In Faro, the melt quantity is still of two orders of magnitude lower than expected in a real accident (e.g. TMI-2), but it is one order of magnitude higher than what has been experimentally performed so far in the field using real corium material. Furthermore the depth of water (up to 2m), the system pressure and temperature (up to 10 MPa and 573K), the melt delivery conditions (flow rate, release by gravity) are realistic and the volumes involved scale the reactor case. The test facilities for Faro experiments are shown in Figure 4.

So far, high pressure core melt down scenarios have been simulated. Two preliminary tests known as L-06 and L-08 were performed with 18 and 44 kg of pure oxide UO_2 and ZrO_2 melts poured into 1-m depth water at saturation at 5.0 MPa (537K) from a nozzle of diameter of 100mm. They have shown that, although significant breakup and thus quenching of the melt occurred, part of the corium (1/3) reached the bottom plate still molten. Nevertheless, the thermal load on the bottom plate remained rather mild with a temperature increase of the contact face around 275K.

Two large size tests, known as L-11 and L-14, were performed. They involved, respectively, 151 kg and 125 kg of corium material melts quenched in 500kg, 2-meter depth water at saturation at 5.0 MPa. These tests, together with the two preliminary tests, allow quantifying

the effect of melt mass, H_2 generation and water depth on the quenching process. The pressure histories of the tests L-06, L-08, L-11, and L-14 are shown in Figure 5.

KROTOS Experiments

The KROTOS facility (shown in Figure 6) was used for energetic FCI studies in the molten UO_2/ZrO_2 and water system in conjunction with large scale FARO test. The objective of the test is to investigate the premixing of molten fuel jets with nearly saturated water and subcooled water mainly in 1-D geometry. The potential for the energetic interaction is also studied. During every experiment the dynamic pressurization of the test section and pressure vessel, as well as the water and cover gas temperatures, and water level swell are measured. Post-test debris analysis was also performed for the additional information about explosion efficiency. Until recently, explosive interaction has not been observed with the corium material. Minor propagation wave, however, was observed with the test section pressure of about 2 bar. [35]

3. Vapor Explosion Modelling

In this chapter, existing models for vapor explosions are reviewed. There are basically three modeling approaches which can be used to assess the consequences of vapor explosions.

1) Thermodynamic models

2) FCI parametric models

3) Direct simulations of the FCI based on mechanistic modelling

The first approach only provides an estimate for the efficiency of a vapor explosion. The mathematical details of this approach are provided in Section 3.1. The limitation of this approach is that one is required to provide the global values of the fuel involved in the explosion, the vapor void fraction, and the amount of coolant participating in the explosion. The results of these analyses indicate that for reasonable ranges of fuel to coolant mass ratios and global void fractions, the predicted conversion ratios and explosion pressures are more than an order of magnitude higher than those observed experimentally. Hence, such analyses are not useful for design calculations. Nevertheless, the review provided in Section 3.1 provides an historical perspective on vapor explosion modeling and the underlying assumptions.

The second approach is more mechanistic since it involves the use of models that allow for kinetics between the fuel and the coolant liquids and thereby provide more realistic estimates of the energy transfer rates. However, such models are generally parametric in nature [36]; one is still required to specify the amount of coolant and fuel participating in the explosion. This is not known *a priori* unless more mechanistic mixing analysis is performed. Also, these models are lumped parameter models that require estimates of the global mixture vapor void fractions. Thus, as in the thermodynamic model, the fuel to coolant liquid ratio in the explosion mixture

and the global void fraction are the key determinants for the explosion pressure history. The results from these parametric calculations would provide not only the peak pressure (as would the thermodynamic models), but also the time history of the pressure. These estimates are not as conservative as the thermodynamic approach; however, they still suffer from being parametric and lack any dimensionality.

The final approach is to mechanistically consider the different phases of the FCI (i.e. mixing, triggering, propagation, and expansion). Since different physical processes govern each of the four phases of the explosion, earlier work on each phase will be reviewed separately. Section 3.2 through 3.6 summarize earlier parametric and mechanistic models for each of the four phases.

3.1 Thermodynamic Models of Vapor Explosions

In the thermodynamic analysis of steam explosions, the equilibrium pressure, the work potential and the mass of steam are predicted in a two step process. In the first step, the melt and coolant achieve thermodynamic equilibrium in an adiabatic, constant volume process. During the second step, the work potential of the interaction is determined based on the assumption that either the melt and coolant expand isentropically to a final prescribed state, or the fluid surrounding the explosion zone is compressed isentropically by the expanding fuel/coolant mixture. In what follows, the details of the analysis for the assumed isentropic expansion of the explosion mixture are presented. The alternative approach based on assuming an isentropic compression of the surrounding fluid can be formulated similarly.

To determine the equilibrium temperature, the change in the internal energy for each component of the mixture (fuel and coolant) can be expressed as:

$$\Delta I_c = m_c c_{v,c} (T_e - T_{c,1}) \qquad (1)$$

$$\Delta I_f = m_f c_{v,f} (T_e - T_{f,1}) \qquad (2)$$

where ΔI is the change in the internal energy, m is the mass, c_v is the specific heat at constant volume, and T is the temperature. The subscripts c,f,e and 1 refer to coolant, fuel, equilibrium condition, and initial state, respectively. It has been assumed in the formulation of above equations that there is no heat or work transfer to the surroundings, the changes in potential and kinetic energies are negligible, and the changes in specific heats with temperature are also negligible. The equilibrium temperature is obtained by equating the changes in the total energy of the fuel and coolant to zero:

$$T_e = \frac{T_{c,1} + (m_f\, c_{v,f} / m_c\, c_{v,c})\, T_{f,1}}{1 + m_f c_{v,f} / m_c c_{v,c}} \qquad (3)$$

In the second step, the fuel-coolant mixture is assumed to expand isentropically to the final state [37]. The final state is either a specified volume or pressure. In reactor cavities with large volumes of water, the final state is specified by the pressure. Since the coolant and fuel are prescribed to remain in thermal equilibrium, the entropy of the coolant increases and the entropy of the fuel decreases. During the expansion process, the coolant passes into the two-phase region and the final state of the coolant may be superheated vapor. The fuel, however, remains in a subcooled state during this process. In this analysis, the control mass includes the fuel-coolant mixture. From the first law of thermodynamics, the work is computed by considering the change in the internal energy of the mixture,

$$\begin{aligned} W_{net} &= -m_m \Delta u_m = -(m_c \Delta u_c + m_f \Delta u_f) \\ &= -\left[m_c (u_{c,2} - u_{c,e}) + m_f (u_{f,2} - u_{f,e})\right] \end{aligned} \qquad (4)$$

where the subscript m and 2 refer to the mixture and final state of the mixture, respectively.

The specific internal energy is defined as:

$$u = c_v (T - T_{ref}) + x\, u_{fg} = c_v (T - T_{ref}) + x(h_{fg} - p v_{fg}) \qquad (5)$$

where x is the quality, and T_{ref} is a reference (datum) temperature. Equation (4) can now be

written as:

$$W_{net} = m_c\left[c_v(T_e - T_2) + x_e(h_{fg} - pv_{fg})_e - x_2(h_{fg} - pv_{fg})_2\right]_c + m_f\left[c_v(T_e - T_2) + x_e(h_{fg} - pv_{fg})_e - x_2(h_{fg} - pv_{fg})_2\right]_f \quad (6)$$

The efficiency of the process (conversion ratio) can be defined as the ratio of the net work to the thermal energy of the fuel, and using this definition, the net work becomes:

$$W_{net} = CR\ \ m_f\ c_{v,f}\left(T_{f,1} - T_{c,1}\right) \quad (7)$$

where *CR* is the conversion ratio.

For the isentropic expansion of the mixture, the change in the entropy of the mixture is zero, therefore,

$$T_m ds_m = dh_m - v_m dp_m = 0 \quad (8)$$

The mixture enthalpy and specific volume can be written as:

$$h_m = \frac{(m_c c_{p,c} + m_f c_{p,f})(T - T_{ref}) + m_c x h_{fg,c}}{m_c + m_f}$$
$$v_m = \frac{x\, m_c\, v_g}{m_c + m_f} = \frac{x\, R_c T}{p}\frac{m_c}{m_c + m_f} \quad (9),(10)$$

where R_c is the coolant gas constant and the subscript g refers to the coolant vapor. In writing Eqn(10), it has been assumed that the specific volumes of the fuel melt and liquid coolant are negligible in comparison to the coolant vapor, and the perfect gas law applies to the coolant vapor.

Differentiating Eqn(9) yields:

$$dh_m = \frac{(m_c c_{p,c} + m_f c_{p,f})\, dT + m_c h_{fg,c}\, dx}{m_c + m_f} \quad (11)$$

The change in the pressure can be calculated using the Clausius-Clapeyron equation and assuming that the equilibrium state is close to the saturation line and the expansion occurs in the two-phase region, therefore,

$$dp_m \cong \left.\frac{\partial p}{\partial T}\right|_{sat} dT = \frac{h_{fg,c}}{T v_{fg,c}} dT \cong \frac{p\, h_{fg,c}}{R_c} \frac{dT}{T^2} \qquad (12)$$

Substituting Eqns (10),(11), and (12), into Eqn(8) yields:

$$(m_c c_{p,c} + m_f c_{p,f}) \frac{dT}{T} + m_c h_{fg,c} d\left(\frac{x}{T}\right) = 0, \qquad (13)$$

and integration of this equation between the equilibrium state and the final

state gives:

$$x_2 = T_2 \left[\frac{x_e}{T_e} + \frac{m_c c_{p,c} + m_f c_{p,f}}{m_c h_{fg,c}} \ln \frac{T_e}{T_2} \right] \qquad (14)$$

Once the final quality is obtained, the final mixture temperature can also be determined. If the final quality is less than 1, the final coolant state is in the two-phase region. If x_e is greater than 1, the final coolant state is superheated. Under this condition, Eqns (10) and (11) can be written as:

$$v_m = \frac{R_c T}{p} \frac{m_c}{m_c + m_f}$$
$$dh_m = \frac{(m_c c_{p,c} + m_f c_{p,f}) dT}{m_c + m_f} \qquad (15,16)$$

Substituting of Eqns (15) and (16) into Eqn(8) yields:

$$\frac{m_c c_{p,c} + m_f c_{p,f}}{m_c R_c} \frac{dT}{T} = \frac{dp}{p} \qquad (17)$$

Integration of the Eqn(17) between the equilibrium and final states gives:

$$T_2 = T_e \left(\frac{p_2}{P_e} \right)^{\frac{m_c R_c}{m_c c_{p,c} + m_f c_{p,f}}} \qquad (18)$$

where p_2 is the cavity pressure, and the equilibrium pressure p_e is obtained from:

$$\begin{aligned} p_e &= \rho_e R_c T_e \\ \rho_e &= \rho_{c,1} \end{aligned} \qquad (19)$$

assuming ideal gas behavior, and constant volume heating of the gas.

Therefore, given the mass of fuel and coolant participating in the explosion together with the fuel and coolant initial conditions, the thermodynamic analysis yields the upper bound values for the pressure and work potential during the expansion. Generally these values are more than an order of magnitude higher than those observed experimentally. Hence, such analyses are not appropriate for design or safety assessment calculations.

3.2 Premixing Phase Models

In this phase, interpenetration between the high temperature melt and the cold liquid takes place, leading to a metastable configuration. Two types of configurations between hot melt and cold liquid can be considered. The first configuration is a case where hot melt ``globules'' are dispersed within a continuous cold liquid, and the other is the opposite situation. The first case represents most of the situations observable in hypothetical accidents in nuclear reactors, and, therefore, are mainly considered in this report. The latter case represents accidents experienced in the foundry industries where volatile liquids such as water may be introduced into high temperature melt.

For the first configuration mentioned above, the melt which has higher density flows under gravity into the coolant and a coarse mixture of the two liquids is produced. Due to film boiling around the hot melt, a vapor film will separate the hot and cold liquids maintaining a metastable configuration. The premixing phase can, depending upon the geometry and inlet

velocity of the melt, last for a small fraction of a second to more than 1 second. During that time the fuel and coolant mixture volume expands. In this stage, thermal interactions between the melt and coolant are relatively insignificant due to the existence of the vapor film separating the two liquids.

The importance of the premixing phase can be appreciated considering the fact that the potential mechanical energy produced for a given thermal energy from the melt strongly depends upon the melt/coolant ratio. This will be demonstrated by parametric and sensitivity calculations, to be discussed in chapter 4 of this thesis.

Analysis of the premixing phase involves complex hydrodynamic processes, the details of which are not fully understood. Most vapor explosion models therefore assume known premixed conditions.

Early attempts at quantifying the growth of the fuel-coolant mixture includes the empirical correlations by Corradini and Moses [38]. These authors developed a set of empirical correlations for the time dependent growth of fuel-coolant mixing volume, volume fractions of melt, coolant and vapor, and melt particle diameter. The transient behavior of the mixture was described using the following two dimensionless parameters:

$$T^{+} = \frac{V_F\, t}{D_{F_0}} \left[\frac{\rho_L}{\rho_F} \right]^{1/2} \qquad (20)$$

$$T^{*} = T^{+}\, We^{-\frac{1}{4}} \left[\frac{\rho_F}{\rho_F - \rho_L} \right]^{1/4} \qquad (21)$$

where V_F is the fuel velocity, D_{f0} is the initial melt diameter, and We is the Weber number defined as:

$$We = \rho_L\, D V^2 / \sigma \qquad (22)$$

where ρ_L is coolant density and D, σ, and V are diameter, surface tension, and velocity of the melt droplet, respectively. Both T^+ and T^* were claimed to adequately correlate the data. If Taylor instabilities are the dominant mixing mechanism, T^* may provide a more general formulation. The dependent mixing variables were correlated as a function of the dimensionless time as given by the following expressions:

$$V_{mix} = \frac{3 M_F}{\rho_F} (T^+)^2 \qquad (23)$$

$$\alpha_F = \frac{1}{3(T^+)^2} \qquad (24)$$

$$\alpha_v = \frac{1}{2} - \frac{1}{3(T^+)^2} \qquad (25)$$

$$\alpha_L = 1 - \alpha_F - \alpha_v \qquad (26)$$

$$D_F = D_{F_0} e^{-T^+} \qquad (27)$$

where α_F, α_v, and α_L represent the volume fractions of the molten material, vapor, and liquid coolant, respectively. The correlations are based on the results of FITS data reported in detail by Berman [34,35,39,40,41] It should be noted that the above correlations are not valid for small T^+ where a negative vapor volume fraction may be calculated.

Subsequently, Chu and Corradini [42,43] developed a theoretical model for the break up by Rayleigh-Taylor instability of melt particles. This model predicts an exponential decrease of drop diameter with the dimensionless time as follows.

$$D(T^+) = D(0) \exp\left[-C \, We^{0.246} \left(T^+\right)^{0.772} \right] \qquad (28)$$

where T^+ is again the dimensionless time defined in Eqn(20), and C is given by:

$$C = 0.1708 - 0.149\sqrt{\rho_L / \rho_F} \qquad (29)$$

Figure 7 shows the dimensionless droplet diameter decreasing with the

dimensionless time for different Weber numbers.

Phenomenologically-based computer models for premixing have been developed by Corradini and Moses [38], Bankoff and Han [44], Han and Bankoff [45], Chu and Corradini [43], and Abolfadl and Theofanous [46].

In the model developed by Corradini and Moses [38], time-dependent mixing was simulated in the pouring mode of contact. The falling melt was represented by Lagrangian material volumes which fall through the gas atmosphere into a coolant water pool. This model approximates two-dimensional effects by allowing radial expansions. Mass and energy balances were considered. However, the momentum equations were not solved. Instead, the empirical mixing correlations described above (Eqns (20) through (27) were utilized for the dynamic dispersion of the fuel. The model was able to predict the rate of vapor and hydrogen generation as the fuel mixed with water. Sample calculation for Sandia FITS experiment showed that the amount of hydrogen generated was very small.

Bankoff and Han [44] suggested a quasi-steady one-dimensional model for mixing. The one-dimensional mixing model assumes a complete failure of the lower support plate resulting possibly from a preliminary explosion near the top of the pool. The fuel particles were considered as spheres of uniform size which did not undergo breakup as they mixed with the coolant. In dealing with the hydrodynamic effects, both homogeneous and two-fluid models were used. Their results indicated that the void fraction rose rapidly to above 0.85 while the fuel particle volume fraction decreased sharply. In a later publication, Han and Bankoff [45] used the one-dimensional multiphase code PHOENICS [47] to model time-dependent mixing of molten core material with the lower plenum water pool in a PWR. Water and vapor were treated as a homogeneous mixture, while fuel drops were considered as a second fluid, solving mass, momentum and energy equations. The model also assumes that: (1) the water is initially at saturation temperature, (2) the fuel drop temperature remains constant, (3) the fuel drops are

equal in diameter and spherical in shape, and (4) the ambient pressure is constant throughout the mixing process. A cylindrical coordinate system with axisymmetry was used for the geometry of 3 m in diameter and 2 m of initial height of water. Figure 8 shows the penetration of fuel drops and growth of void fraction within the water. It is seen from this figure that the penetration of fuel drops progresses very slowly and that most of the fuel drops are present in the region where the void fraction is greater than 0.6 in less than 0.5 sec.

In the model developed by Chu and Corradini [43], the breakup of fuel droplets during mixing was modeled. This model utilized the one-dimensional transient Lagrangian-Eulerian Code TEXAS [48]. The coolant vapor and liquid were represented by two Eulerian fields, and the fuel particles by a Lagrangian field. The fuel diameter history was determined by the correlation based on the relative-velocity fragmentation model by Chu and Corradini [42](Eqns (28) and (29)). This model, being one-dimensional, over-predicts the hydrodynamic interaction between the generated vapor and the falling fuel particles.

By modifying the transient two-dimensional version of the K-FIX computer code (Rivard and Torrey [49,50], Abolfadl and Theofanous [46] modeled premixing in an axisymmetric cylindrical geometry, where venting through the downcomer inlet could be considered for mixing in a PWR lower plenum as shown Figure 9.

In this model the momentum conservation equations represent a two-fluid mixture where coolant liquid and vapor were treated as a single fluid, and fuel was considered as a separate fluid with a predetermined ``globule" size (2 cm). No further breakup was considered throughout the calculation. The fuel temperature was assumed to remain unchanged during the transient. However, heat transfer between the fuel and coolant was modeled by using steady-state heat transfer correlations. Both radiative and convective heat transfer were considered for the fuel/water interface; the radiative mechanism was neglected for fuel/gas. The calculated distributions of volume fraction of fuel and coolant for 0.5 and 1.0 second are shown in Figure

10 which clearly indicate the depletion of water within the major portion of the fuel pour.

In a follow-up work, Amarasooriya and Theofanous [51] improved the same model by providing separate momentum conservation equations for coolant liquid and vapor phases, which allowed vapor/water slip. Also, temperature change of the fuel particles was taken into account by employing the energy equations for the fuel phase. For numerical simulation they used their computer code build around K-FIX solver [49] for the same geometry configuration shown Figure 9 for a typical reactor. It was found that allowing steam/water slip in the improved model did not affect the qualitative behavior of the premixing transient. Neither one of the calculations, however, was compared against experimental data. Nevertheless, the calculations clearly show the significance of multidimensional expansion of the fuel-coolant mixture which was not obvious in previous works.

3.3 Triggering and Fragmentation

In this phase of vapor explosion, at some point in the mixture, the meta-stable state present during the coarse mixing phase is transformed to a liquid-liquid contact between the melt and coolant phases. Direct contact between the melt and coolant takes place when the vapor film, which separated them during the coarse premixing phase, is disrupted. The disruption can be spontaneous, for example due to the impaction of the melt-coolant mixture with a rigid body, or it can be externally-imposed. Direct contact between the melt and coolant is accompanied by violent heat transfer, evaporation of the coolant, and fragmentation of the melt.

The timing of triggering is important since the details of the propagation and expansion phases which follow depend on the mixture conditions at the time of triggering (Condiff [52], Medhekar et al. [53]). For example, early trigger may occur before complete hot melt entry or with poor coarse mixing condition resulting in a small explosion. On the other hand, a late triggering may find the mixture in a stratified geometry or partially solidified melt. The location of triggering also is considered to play an important role for the prediction of subsequent

dynamics.

The timing and location of triggering in a coarse mixture are, however, difficult to predict due to uncertainties in the many random processes which can lead to a local disruption of the vapor film separating the melt-coolant phases. No theoretical or experimental evidence is currently available for prediction of triggering initiation. Parametric representation of triggering appears to be the most plausible method at this time. In the triggering-propagation model of Medhekar et al. [53], (to be reviewed below), triggering is imposed in a user-specified location, or node in the computational mesh, by assuming a sudden establishment of direct contact between the melt and coolant phases.

3.4 Fragmentation Mechanism

Fine fragmentation of the hot liquid, resulting in a dramatic increase of the liquid surface area, is the main mechanism for rapid heat transfer to the coolant. Fragmentation mechanisms can be classified into either hydrodynamic or thermal mechanisms. Hydrodynamic fragmentation models assume that fragmentation of the molten drop occurs due to purely hydrodynamic forces when the relative velocity between the two liquids is high. The velocity difference is generated either due to the initial entry or when the two species, having different densities, are accelerated by a shock wave front. On the other hand, in thermal fragmentation, forces directly related to heat transfer, coolant evaporation and pressure generation are assumed to dominate. It should be noted, however, that both of these mechanisms can possibly act simultaneously.

Hydrodynamic Fragmentation

Hydrodynamic fragmentation is believed to involve several types of mechanisms such as Rayleigh-Taylor instability, Kelvin-Helmholtz instability, and boundary layer stripping. According to the Rayleigh-Taylor instability, when the two fluids sharing a common interface

plane boundary are accelerated in a direction from the lighter liquid to the heavier one, irregularities of the interface develop. Kelvin-Helmholtz instability addresses the unstable interface in a liquid-liquid system. In boundary layer stripping, the tangential component of the flow at the interface of the drop surface exerts shear forces which set the boundary layer in motion.

Hydrodynamic fragmentation of drops can occur generally in two integral ways. The first case will be when the drop is accelerated rapidly through the surrounding media. The other situation, which is more dominant in the propagation phase of vapor explosion, is when a shock wave moves through the liquid and impacts the droplets. In the latter case, the inertia force is high enough to overcome the cohesive force of the drop surface tension. The ratio between these two forces can be represented by the Weber number defined in Eqn(22). Experimentally, Ivins [54] found increased fragmentation when the Weber number exceeds the critical value (between 10 and 20) for low melting-point metals (tin, lead, bismuth, and mercury). Other similar experiments, however, show that the thermal effects also influence the fragmentation and may override hydrodynamic effects. The experiment with mercury into water, reported by Bradley and Baker [55], indicates that heated liquid jets can yield much higher breakup. Considering the high melt temperature (1800 to 3500 K) and low coolant critical point (T_{cr}=647 K) in the LWR accident environment, it is not likely that the fragmentation process is controlled by the hydrodynamic mechanism alone.

Thermal Fragmentation

Swift and Baker [56] postulated that boiling results in the breakup of the fuel drops by the formation and collapse of vapor bubbles at the surface of the drops. They were the first to hypothesize that fragmentation might occur in transition and nucleate boiling regimes where the boiling is hydrodynamically violent. An indication of the boiling violence is given by the maximum bubble work potential W_B:

$$W_B = \frac{4}{3}\pi R_B{}^3 |\Delta P| \qquad (30)$$

where R_B is the maximum bubble radius and ΔP is the difference between the bubble and ambient coolant pressures.

The violent boiling fragmentation hypothesis seems to be consistent with the experimental observation by Swift and Pavi [1], where Al, U, Ni, Zr, and steel fragmented in sodium but not in water. The melting points of these metals are all above the critical point of water (373 °C). Sodium, on the other hand, has a boiling point of 882 °C and a critical temperature of 2300 °C, so that all of these metals were still molten in the region of violent boiling. It should be noted that this temperature criterion was not satisfied for other experiments where large quantities of molten metals were poured in water by Long [57], Briggs [26], and Fry and Robinson [27].

Early experimental work such as that performed by Long [57] shows that a small amount of cold liquid trapped inside of the hot phase resulted in explosive interactions. Based on this observation, Schins [58] proposed the following sequence for fragmentation by coolant entrapment by hot liquid as follows:

1) Direct liquid-liquid contact, resulting in high heat transfer to nearby coolant layer,

2) Incipience of transition boiling, which imparts a shock to the hot liquid,

3) Collapse of the vapor film, which initiates cavitation of bubbles within the hot liquid,

4) Entrapment of coolant in such cavitated hot liquid, and

5) Fragmentation due to the rapid volume expansion, by boiling, of entrained liquid within hot liquid

Corradini [59] proposed a thermal fragmentation model based on Taylor instability. The work was performed in an overall effort to model Sandia steam explosion experiments. In this

model, trigger-induced vapor film collapse causes the fuel and coolant to come in near contact. Direct contact was assumed unlikely because of substantially large temperature difference between hot and cold liquids such that the interface temperature is much higher than the critical point of the water coolant. Rapid generation of vapor was considered to cause acceleration of both fuel and coolant liquid. A schematic diagram of the Taylor instability in this model is shown in Figure 11. The cyclic process continues as the fragmented fuel is quenched, causing the vapor pressurization, Taylor instabilities, and further fragmentation as shown in Figure 12.

The mass of the fragmented fuel, during the near contact was assumed to be that mass contained in the wavelets of the distorted fuel surface (Figure 11). The wavelet was assumed to be cone shape. A quantitative analysis was made to estimate the mass fragmentation rate as shown bellow.

$$FR = \left[\frac{\rho_F \lambda_{m_f} A_{fr}}{3\tau_{\exp}} + 4\rho_F A_{fr} \sqrt{a_F(t)\lambda_{cr}(t)} \right] \frac{6\alpha_3}{\pi D_F{}^3} \qquad (31)$$

where ρ_F is density of fuel melt, D_F is diameter of the fuel drop, and A_{fr} stands for the area of near contact. The other parameters are defined as:

$$\tau_{\exp} = \left(\frac{2\delta}{a_F} \right)^{1/2} \qquad (32)$$

$$a_F(t) = \frac{P_c/4 - P_v}{\rho_F D_F(t)} \qquad (33)$$

$$\lambda_{m_f} = 2\pi \sqrt{\frac{3\sigma_F}{(\rho_F - \rho_c) a_F(t)}} \qquad (34)$$

and the critical wavelength is

$$\lambda_{cr}(t) = 2\pi \sqrt{\frac{\sigma_F}{(\rho_F - \rho_v) a_F(t)}} \qquad (36)$$

Empirical estimations were made for the area of near contact, A_c

A thermal fragmentation model based on coolant jet penetration and entrapment was suggested by Board et al. [60] In this model, high speed coolant formed by vapor collapse penetrates and disperses in the melt; subsequent evaporation of the entrapped coolant causes melt fragmentation. Nelson et al. [15] obtained photographic evidence of bubble collapse and jet formation and showed tiny droplets of water totally enclosed within the melt. They postulated that steam bubbles produced by thermal interaction between the melt and water as well as cavitation bubbles produced by pressure disturbance in the water can collapse to produce jets.

A similar model was proposed by Kim and Corradini [61] as a coolant jet penetration model. In this model, the fragmentation is conceptually divided into four stages as shown in Figure 13, the last three of which occur cyclically.

1) Film boiling occurs between coolant and fuel interface.

2) Due to some triggering mechanism such as shock wave, filmcollapse and coolant jet formation occur. The interface becomes unstable during the collapse and regrowth of the vapor film.

3) Jet penetration and entrapment of the coolant occurs. Under certain conditions, the jets with enough speed contact fuel surface and even penetrate the melt, which forms a mixture of vapor and coolant drops entrapped in the fuel.

4) Rapid evaporation of entrapped coolant occurs, causing the outer portion of the fuel to separate from the parent fuel droplet and form a molten fuel shell surrounded on either side by a vapor film. The molten fuel shell expands and breaks up by the instabilities growth on the surface.

3.5 Propagation Phase Models

The thermal and hydrodynamic processes initiated by the triggering event propagate through the coarse fuel-coolant mixture. A "thermal detonation front" moves through the coarse mixture with supersonic velocity. Behind the front, the fuel is partially fragmented into particles typically 100 microns in diameter. The fragmentation is mainly due to hydrodynamic instability of the fuel melt caused by the enormous pressure and velocity gradients behind the detonation front. The fragmented particles rapidly approach thermal equilibrium with the coolant due to their large specific surface areas. Momentum equilibrium between the different phases (unfragmented fuel, liquid coolant and vapor), however, is achieved relatively slowly in comparison with the fragmentation and heat transfer processes.

Early attempts in modeling fuel-coolant explosions were based on an assumed analogy with the classical one-dimensional chemical detonation (Board et al. [62]). Due to the significance of this analogy, it will be explained below in some detail.

Figure 14 represents a schematics of chemical and vapor explosion fronts. In one-dimensional chemical detonation, a plane detonation wave is assumed to be established in an infinitely large explosive medium. The detonation front moves with a constant velocity, supersonic with respect to the unexploded mixture (V_1 in Figure 14a), and is followed by a zone of chemical reaction, where complete reaction leading to thermodynamic equilibrium takes place. The reaction zone itself is separated from the products zone by a plane (X_1 in Figure 14a). By using thermodynamic arguments it can be shown that, for a stable detonation front, the relative velocity of the plane X_1 with respect to the detonation front must be equal to the local sonic velocity at X_1 (See, for example Taylor [63]). Although the reaction zone expands with time, its velocity, pressure, etc. profiles remain self similar. The jump associated with the chemical process in the reaction zone can be represented with fluid mass, momentum and energy conservation equation as:

$$V_1 / v_1 = V_2 / v_2 \qquad (37)$$

$$\frac{V_1^2}{v_1} + P_1 = \frac{V_2^2}{v_2} + P_2 \qquad (38)$$

$$U_1 + \frac{1}{2}V_1^2 + P_1 v_1 = U_2 + \frac{1}{2}V_2^2 + P_2 v_2 \qquad (39)$$

The above three equations, as noted, include four unknowns, P_2, U_2, v_2, and V_2, representing the pressure, specific internal energy, specific volume, and velocity of the products. In these equation P_1, U_1, v_1, and $V_{w,1}$ represent the same quantities in the unexploded zone. These equations can be combined to get the Rankine-Hugoniot

relation:

$$U_2 - U_1 = (P_1 + P_2)(v_1 - v_2)/2 \qquad (40)$$

An additional equation is provided by the products equation of state in the form of

$$U_1 = U_1(P_1, v_1)$$

The Rankine-Hugoniot (R-H) equation thus represents the relation between P_2 and v_2 for a set of known unexploded mixture conditions (P_1, v_1), and has the general form depicted in Figure 15 (Board et al. [62]), which does not pass through the (P_1,v_1) point. The condition of sonic velocity at plane X_1_ provides an additional equation which closes the equation set of Eqns (36) to (39). It can be shown that the sonic velocity at X_1 represents point O in Figure 15 which is called the Chapman-Jouguet (C-J) point. Thus, for a 1-D, steady state chemical detonation, the propagation velocity of the detonation front, and the other physical quantities defining the detonation process such as the detonation pressure and temperature, the specific volume of the products and their streaming velocity behind the detonation wave, are assumed unique functions of the properties of the unexploded zone. Details of the chemical processes which take place in the reaction zone are not considered in the theory, as long as the final products and their equations of state are known. This is justified since the reaction zone in a chemical explosion is typically only a fraction of a millimeter in thickness.

An analogy between thermal and chemical explosions was first suggested by Board et al. [64]. According to this model, schematically depicted in Figure 16 (Board et al. [62]), immediately behind the front the large velocity differential between fuel and coolant causes fragmentation of the fuel, which in turn brings about efficient heat transfer between the fragmented fuel and coolant. Thermodynamic equilibrium is achieved at the C-J plane, although the fragmentation process may continue over some distance behind the C-J plane. Since the flow is assumed homogeneous, the zone between the detonation front and the C-J plane represents the reaction zone, and is self similar. The fact that thermodynamic equilibrium is reached before complete fragmentation is not inconsistent with the hydrodynamic detonation theory, and can happen in chemical detonation processes involving a two-phase unexploded mixture (Taylor, [63]). In order for hydrodynamic detonation theory to be applicable, the following condition must be valid

$$t_{ht} << t_b << t_r, \qquad (41)$$

where t_r is the characteristic time associated with the achievement of velocity equilibrium, t_b the characteristic breakup time of fuel particles, and t_{ht} is the characteristic time associated with thermal equilibrium of fragmented fuel with the coolant. Using an empirical correlation for the break-up time of a particle behind shock fronts suggested by Simpkins and Bales [65], Board et al. showed that Eqn(41) is indeed valid in vapor explosions. Board et al. [62] further argued that the 1-D analysis is valid in any explosion when the region of coarse intermixing is large compared with the reaction range (about 10 cm according to 1-D detonation model), and where the reaction front is approximately planar on a scale of many times its thickness. However, in a vapor explosion the fuel fragmentation is usually incomplete, the unexploded mixture often contains vapor (two-phase coolant intermixed with fuel), and the decay of slip velocity between the coolant and unfragmented fuel behind the detonation front is relatively slow. As a result the assumption of homogeneous equilibrium explosion products, which provides for a unique explosion front velocity, is invalid. Noting these points, Sharon and Bankoff [66] studies the

1-D propagation of a detonation front in a coarse-mix with and without velocity equilibrium between coolant-unfragmented fuel behind the detonation front. Starting from two-phase (unfragmented fuel as one phase, and coolant and fragmented fuel as the other) mass, momentum, and energy conservation equations, they examined the necessary conditions for the establishment of a steady state detonation front. They showed that the C-J plane conditions are not unique for a multi-phase detonation involving an incomplete fragmentation.

Condiff [52] further extended the analysis of Sharon and Bankoff [66] and considered an unexploded mixture containing a two phase (vapor and liquid) coolant. They showed that, depending on the vapor volume fraction in the unexploded mixture, a wide spectrum of permissible C-J states were possible, indicating a further limitation on the steady-state detonation front movement assumption.

Medhekar et al. [53] modeled the propagation phase of a vapor explosion by direct numerical solution of transient conservation equations. The conservation equations were three phases (coolant liquid, coolant vapor, and unfragmented fuel), two fluid (unfragmented fuel, and debris-coolant mixture). Fragmented fuel debris, coolant liquid and coolant vapor were thus assumed to have the same velocity. The debris was assumed to reach thermal equilibrium with liquid coolant instantaneously following fragmentation. The fuel temperature was assumed to be constant. Thermodynamic non-equilibrium between coolant liquid and vapor, however, was modeled. The interfacial heat transfer and drag among the three phases were calculated using steady-state correlations. Fragmentation kinetics were calculated using the Reinecke-Waldman model [67]. The model suggests a non-linear breakup kinetics where the rate of fragmentation depends on the relative velocity, ratio of the density of the phases, and the time elapsed since the inception of the shock wave. The fragmentation rate is given by

$$FR = \frac{3}{4}\frac{(1-\theta)}{\pi r^3}\frac{\pi}{4T_b}\frac{U_{rel}}{r}\sqrt{\frac{\rho_c'}{\rho_F'}}\, m_0 \sin\left\{\frac{\pi U_{rel}}{2T_b r}\sqrt{\frac{\rho_c'}{\rho_F'}}\, t\right\} \qquad (42)$$

where T_b is a dimensionless break-up time, and was assumed equal to 1 [53].

The numerical solution scheme was two dimensional and was based on the finite-difference K-FIX code (Rivard and Torrey [49,50]). Medhekar et al.[53] performed simple 1-D calculations to simulate an experiment reported by Baines [68]. In this particular experiment, volume fraction of vapor was available as an averaged (global) value. When numerical simulation was performed in a similar fashion using averaged vapor fraction of 0.2 and fuel volume fraction of 0.2, the comparison was not satisfactory. By noting that the void fraction near the bottom of the experimental setup would be lower than one at the top of the tube, void fraction of 0.1 and fuel volume fraction of 0.4 were tried. Here pressures obtained were 80 to 90 bars and propagation speeds were about 240 m/sec, which are within the experimental data of 50 to 100 bars and 80 to 250 m/sec. The numerical simulation, however, did not simulate non-uniform distribution of initial void fraction. Nevertheless, the model was useful to find the high sensitivity of pressure and propagation speed on the local void fraction. Recently, Ren [69] has developed a mechanistic model based on the solution of transient, three-fluid conservation equations, for the triggering, propagation, and expansion phases. Ren's numerical solution is based on an implicit, point-relaxation technique.

3.6 Expansion Phase Models

The propagation of vapor explosions is so rapid that no significant expansion of the interaction zone occurs before the interaction is completed. In this phase of the vapor explosion, one can observe the highly pressurized zone established by triggering and propagation process eventually expands through the surroundings. The mechanical impact by the vapor explosion on the surroundings can be assessed by completing the analysis of this phase. Hicks and Menzies [37] calculated the equilibrium thermodynamic work for UO_2/Na system. They assumed isobaric heat transfer from the fuel to the coolant, followed by isentropic expansion to a specified ambient pressure while maintaining thermal equilibrium. The results of

their calculations show that the specific work done is maximized at a specified coolant/fuel ratio. The work done and the coolant/fuel mass ratio at which work is maximum increase as the end pressure decreases. Judd [70] calculated the maximum thermodynamic work using an improved model of the equation of state for sodium and obtained about 30% higher than, but with trends similar to, the earlier work of Hicks and Menzies. As seen in Figure 17 a much broader peak was obtained, so that the sodium/fuel ratio is not so important in determining how much work is done. It should be noted that the maximum thermodynamic work gives much higher values than the experimental data.

4. Conclusions

In an effort to understand the phenomenology of steam explosion, extensive studies has been performed. This report presents both experimental and analytical studies on steam explosions. As for the experimental studies, both small scale tests which involved usually less than 20g of high temperature melt and medium/large scale tests where usually more than 1 kg of melt was used were reviewed. For the modelling part of steam explosions, mechanistic modelling as well as thermodynamic modelling was reviewed.

Based on the current observations on the steam explosion phenomenology, it is difficult to make general understanding on the influences of various physical conditions affecting the phenomenon. Extensive experimental studies using prototypical materials such as Uranium would elucidate some of the important mechanisms of steam explosion, and also provide reliable data base for code assessment study.

References

1. Swift, D.L. and Pavlik, J.,"Fuel-Coolant and Cladding-Coolant Interaction Studies." ANL-7125 p187, Argonne National Laboratory,1966

2. Flory, K. and Paoli, R. and Mesler, R.,"Molten Metal-Water Explosion," Chem. Eng. Progress, Vol 65, 12 ,p50—54 Dec.1969

3. Witte, L.C. and Vyas, T.J. and Gelabert A.A.,"Heat Transfer and Fragmentation During Molten Metal/Water Interaction," J. of Heat Transfer, Vol 95, p512--527, 1973
4. Bjornard, T. H. and Rohsenow, W. M. and Todreas, N.E.,"The Pressure Behavior Accompanying the Fragmentation of Tin in Water," Trans. Am. Nucl. Soc. Vol 19, 1974

5. Arakeri, V.H., "An Experimental Study of the Thermal Interaction for Molten Tin Dropped into Water," UCLA-ENG-7502, UCLA, Dec. 1975

6. Dullforce, T. A. and Buchanan, D.J. and Peckover, R. S., "Self-Triggering of Small-Scale Fuel-Coolant Interactions: I-Experiment," J. Physics D., Vol 9, 1976

7. Anderson, R. P. and Armstrong, D. R., "Experimental Study of Small Scale Vapor Explosions in an Aluminum-Water System," ASME, HTD, Vol 19, p31, Nov. 1981

8. Nelson, L. and Guay, K.P., "Suppression of Steam Explosions in Tin and $FeAl_2O_3$ Melts by Increasing the Viscosity of the Coolant," High Temperature-High Pressures, Vol 18, 1986

9. Nelson, L.S. and Buxton, L., "Steam Explosion Triggering Phenomena: Stainless Steel and Corium-E Simulants Studies with a Floodable Arc Melting Apparatus," SAND-77-77-0998, NUREG/CR-0112, Sandia National Lab, 1978

10. Nelson, L. S. and Duda, P. M., "Steam Explosion Experiments with Single Drops of Iron Oxide Melted with a CO_2 Laser," NUREG/CR-2295,SAND-81-1346 R3, Sandia National Laboratory, 1981

11. Nelson, L. S. and Duda, P. M., "Steam Explosion Experiments with Single Drops of Iron Oxide Melted with a CO_2 Laser. Part II. Parametric Studies," NUREG/CR-2718, SAND-82-1105 R3, Sandia National Laboratory, 1985

12. Kim, H., "Single Droplet Vapor Explosion Experiments, The U. of Wisconsin – Madison, 1986

13. McCraken, G.M., "Investigation of Explosions Produced by Dropping Liquid Metals into Aqueous Solutions," 1972 UKAEA Safety Research Bulletin of the Safety and Reliability Directorate, Vol 11, 1973

14. Nelson, H.W. and Norton, C.L., "Method of Preventing Melt-Water Explosions," U.S. Patent No. 3,447,895

15. Nelson, L. S and Duda, P.M. and Froehlich, G. and Anderle, M., "Photographic Evidence for the Mechanism of Fragmentation of Single Drop of Melt in Triggered Steam Explosion Experiments," J. Non-Equilib. Thermodyn. Vol 13, 1988

16. Dowling, M.F. and Ip, M.B. and Abdel-Khalik, S.I., "Suppression of Vapor Explosions by Dilute Aqueous Polymer Solutions," Nucl Sci & Eng., Vol 113, 1993

17. Becker, K.M. and Lindland, K.P., "The Effects of Surfactants on Hydrodynamic Fragmentation and Steam Explosions," KTH-NEL-50, Royal Institute of Technology, Stockholm, Sweden, 1991

18. Groenveld, P. Explosive vapor Formation," Transactions of the ASME, Journal of Heat Transfer, Vol 236, 1972

19. Becker, K.M. and Engstrom, J. and MacBeth, R.V., "Enhancement of Core Debris Coolability," KTH-NEL-51, Royal Institute of Technology, Stockholm, Sweden, May 1990

20. Kippenhahn, C. and Tegeler, D., "A Bubble Growth Experiment for the Determination of Dynamic Surface Tension," AIChE J., Vol 16, p314, 1970

21. Nelson, L.S. and Wong, C.C. and Eatough, M.J. and Vigil, F.J and Szklarz, D.D. and Fuketa, T., "Steam Explosions of Single Drops of Thermite-Generated Melts: 25 and 50 Weight Percent Aluminum-Iron Oxide Initial Mixtures," SAND-90-0511, Sandia National Laboratory, Oct.1992

22. Kowal, M.G. and Dowling, M.F. and Abdel-Khalik, S.I., "An Experimental Investigation of the Effects of Surfactants on the Severity of Vapor Explosions," Nucl. Sci. & Eng. Vol 115, p185—192, 1993

23. Frid, W., "Ex-Vessel Melt-Coolant Interactions in Deep Water Pool: Thirmal-1 Analyses and Surfactant Investigations," Cooperative Severe Accident Research Program Meeting, May 3-7, 1993 Bethesda, MD.

24. Skelton, W.T., "Effect of Additives on the Likelihood and Severity of Vapor Explosions," Nuclear Engineering, Georgia Institute of Technology, 1993

25. Buxton, L. D. and Nelson, L. S. and Benedick W. B., "Steam Explosion Triggering and Efficiency Studies," SAND-79-0261C, Sandia National Lab, 1979

26. Briggs, A. J., "Experimental Studies of Thermal Interactions at AEE Winfrith," Proceedings of the Third Specialist Meeting on Sodium/Fuel Interactions in Fast Reactor, Tokyo, PNC-N-251-76-12, p75, 1976

27. Fry, C. J. and Robinson, C. H., "Experimental Observations of Propagating Thermal Interactions in Metal/Water System," Fourth CSNI Specialist Meeting on Fuel-Coolant Interaction in Water Reactor Safety, Bournemouth UK, p329, April 1979

28. Buxton, L. D. and Benedick W. B., "Steam Explosion Efficiency Studies," NUREG/CR-0947, SAND-79-1339, Sandia National Lab, Nov. 1979

29. Mitchell, D. E. and Corradini, M. L. and Tarbell W. W., "Intermediate Scale Steam Explosion Phenomena : Experiments and Analysis," NUREG/CR-2145, SAND-81-0124, Sandia National Lab, Sep. 1981

30. Mitchell, D. E. and Evans, N. A., "Steam Explosion Experiments at Intermediate Scale: FITS-B Series," Sandia National Lab, NUREG/CR-3983, SAND-83-1057, 1986

31. Berman, M., "LWR Safety Research Program Semiannual Report Oct. 1981- Mar. 1982," Sandia National Lab, NUREG/CR-2841, 1983

32. Berman, M., "LWR Safety Research Program Semiannual Report Apr. 1982- Sep. 1982,"

Sandia National Lab, NUREG/CR-2841, 1983

33. Magallon, D., and Hohmann, H., "Experimental Investgation of 150-kg-scale corium melt jet quenching in water,", Proceedings of the 7th International Meeting on Nuclear Reactor Thermal-Hydraulics, NURETH-7, Sept 1995

34. Magallon, D., and Leva, G., "FARO LWR Program Test L-14 Data Report," Tech note No. I.96.25, JRC, Ispra, 1996

35. Huhtiniemi, H., Hohmann, H., and Magallon, D., "FCI Experiments in the Corium/Water System," Proceedings of the 7th International Meeting on Nuclear Reactor Thermal-Hydraulics, NURETH-7, Sept 1995

36. Oh, M.D. and Corradini, M.L., "A propagation/Expansion Model for Large Scale Vapor Explosions," Nucl. Sci. & Eng., Vol 96, p225-240, 1987

37. Hicks, E.P. and Menzies, D. C., "Theoretical Studies on the Fast Reactor Maximum Accident, ANL-7120, Argonne National Laboratory, p654-670, 1965

38. Corradini, M.L. and Moses, G.A., "A dynamic model for Fuel-Coolant Mixing," International Meeting on Light Water Reactor Severe Accident Evaluation," Cambridge, Mass., p6.3-1, 1983

39. Berman, M., "LWR Safety Research Program Semiannual Report Oct. 1982- Mar. 1983," Sandia National Lab, NUREG/CR-2841, 1984

40. Berman, M., "LWR Safety Research Program Semiannual Report, Apr. 1983-Sep. 1983," Sandia National Lab, NUREG/CR-2841, 1984

41. Berman, M., "LWR Safety Research Program Semiannual Report, Oct. 1983- Mar. 1984," Sandia National Lab, NUREG/CR-2841, 1986

42. Chu, C.C. and Corradini, M.L., "Hydrodynamic Fragmentation of Liquid Droplets," Trans. Am. Nucl. Soc, Vol 47, p306, 1984

43. Chu, C. C. and Corradini, M. L., "One dimensional Transient Model for Fragmentation and

Mixing Analysis," International ANS/ENS Topical Meeting on Thermal Reactor Safety, San Diego, Calif., 1986

44. Bankoff, S.G. and Han, S.H., "Mixing of Molten Core Material and Water," Nucl. Sci. & Eng., Vol 85 p387—395, 1983

45. Han, S. H. and Bankoff, S. G., "An Unsteady One-Dimensional Two-Fluid Model for Fuel-Coolant Mixing in an LWR Meltdown Accident, Nucl. Eng. & Design, Vol. 95, p285-295, 1986

46. Abolfadl, M. and Theofanous, T., "An Assessment of Steam Explosion-Induced Containment Failure, Part II. Premixing Limits," Nucl. Sci. & Eng., Vol 97, p282-295, 1987

47. "PHOENICS A Computer Code by Concentration," Heat and Momentum Limited, Bakery House, 1981

48. Young, M.F., "The TEXAS Code for Fuel-Coolant Interaction Analysis," Liquid-Metal Fast Breeder Reactor Sefety Mtg., Lyon-Ecully, France, 1982

49. Rivard, W.C. and Torrey, M. D., "K-FIX : A Computer Program for Transient Two-Dimensional, Two-Fluid Flow," Sandia National Lab, LA-NUREG-6623, Apr.1977

50. Rivard, W.C. and Torrey, M.D., "PERM: Correctiontions to the K-FIX Code," Sandia National Lab, LA-NUREG-6623 Suppl.," Mar.1978

51. Amarasooriya, W. H. and Theofanous, T.G., "Premixing of Steam Explosions: A Three-Fluid Model," 25th ASME-AIChE National Heat Transfer Conference, Houston, TX, Jul. 1988

52. Condiff, D. W., "Contributions Concerning Quasi-Steady Propagation of Thermal Detonations Through Dispersions of Hot Liquid Fuel in Cooler Volatile Liquid Coolants," Int. J. Heat Mass Transfer, Vol 25, 1, p87—98, 1982

53. Medhekar, S. and Abolfadl, M. and Theofanous, T.G., "Triggering and Propagation of Steam Explosions," ANS Proceeding, 1988 National Heat Transfer Conference, Vol 3, Jul.

1988

54. Ivins, R. O., "Interactions of Fuel, Cladding, and Coolant," USAEC Report ANL-7399, p162-165, Argonne National Laboratory, 1967

55. Bradley, R. and Baker, L., "Explosive Interactions of Molten metals Injected into Water," Nucl. Sci. & Eng., Vol 48 p387-396, 1972

56. Swift, D. and Baker, L., "Reactor Development Progress Report," ANL-7152, Argonne National Laboratory, p87-96, Jan. 1965

57. Long, G., "Explosion of Molten Aluminum in Water - Cause and Prevention," Metal rogress, Vol 71, p107, 1957

58. Schins. H. "The Consistent Boiling Model for Fragmentation in Mild Thermal Interaction-Boundary Conditions," EURATOM Report: EUR/c-IS/699/73e, EURATOM, 1973

59. Corradini, M. L., "Analysis and Modeling of Steam Explosion Experiments," NUREG/CR-2072, SAND-80-2131 R3, Sandia National Laboratory, 1981

60. Board, S. J. and Farmer, C. L and Poole, D. H., "Fragmentation in Thermal Explosions," Int. J. Heat and Mass Transfer, Vol 17, p331-339, 1974

61. Kim, B. and Corradini, M. L., "Modeling of Small-Scale Single Drop Fuel/Coolant Interactions," Nucl. Sci. & Eng., Vol 98, p16-28, 1988

62. Board, S. J. and Hall, R. W. and Hall, R. S., "Detonation of Fuel Coolant Explosions," Nature, 254, p319, Mar. 1975

63. Taylor, J., "Detonation in Condensed Explosives," Oxford at The Clarendon Press, 1952

64. Board, S. J. and Hall, R. W., "Propagation of Thermal Explosions. Part II: A Theoretical Model," RD/B/N-3249, 1974

65. Simpkins, P.G. and Bales, E.L., "Water-Drop Response to Sudden Accelerations," J. Fluid Mech., Vol 55 part IV, p629-639, 1972

66. Sharon, A. and Bankoff, S.G., "On the existence of steady supercritical plane thermal detonations," Int. J. Heat Mass Transfer, Vol 24, p1561-1572, 1981

67. Reinecke, W. G. and Waldman, G. D., "Investigation of Water Drop Disintegration in a Region Behind Strong Shock Wave," Third Int. Conf. on Rain Erosion and Related Phenomena, Hampshire, England, 1970

68. Baines, M., "Preliminary Measurements of Steam Explosions Work Yields in a Constrained System," Proceedings of National Heat Transfer Conference, Leeds, 1984

69. Ren, W. M., "Mechanistic Modeling of Steam Explosions," Ph.D. Thesis, Georgia Institute of Technology," 1994

70. Judd, A. M., "Calculation of the Thermodynamic Efficiency of Molten Fuel-Coolant Interaction," Trans. Am. Nucl. Soc., Vol3(1), p369, 1970

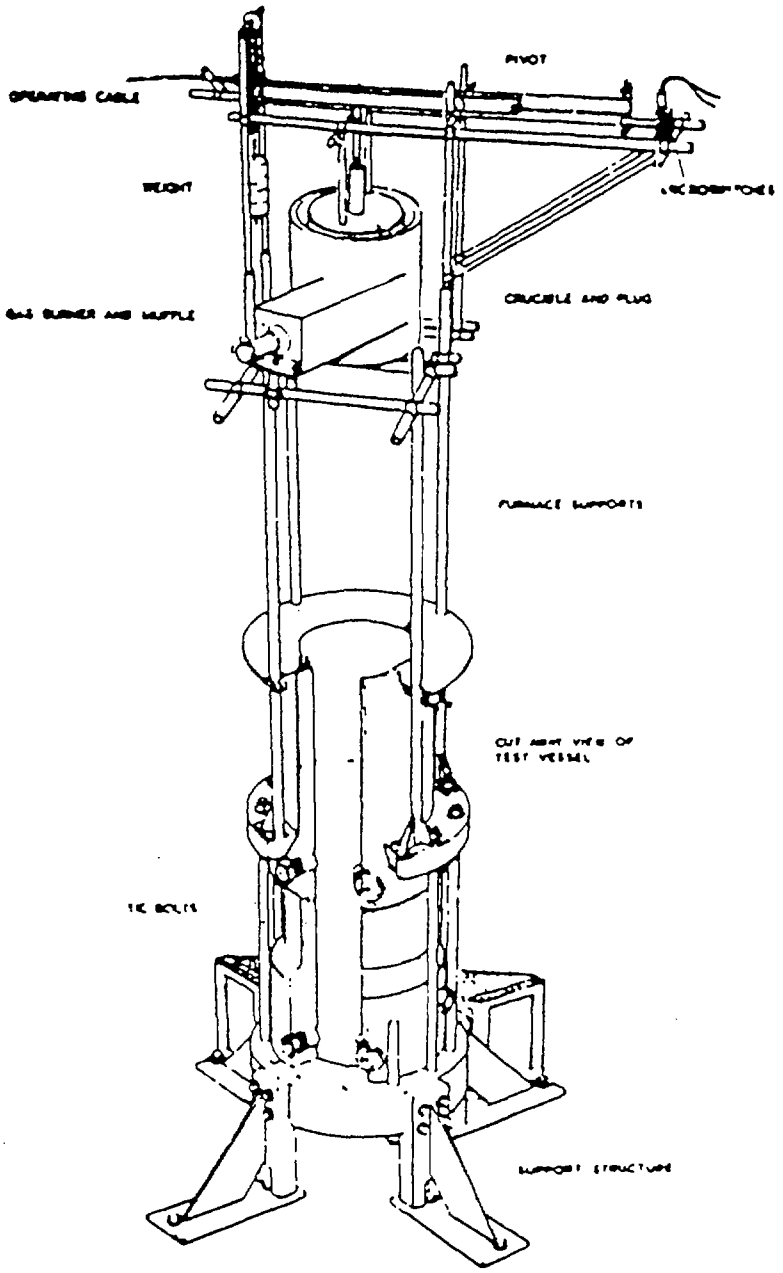

Fig 1. Fig 1. Test Vessel, Furnace, and Release Mechanism. Briggs (1976)

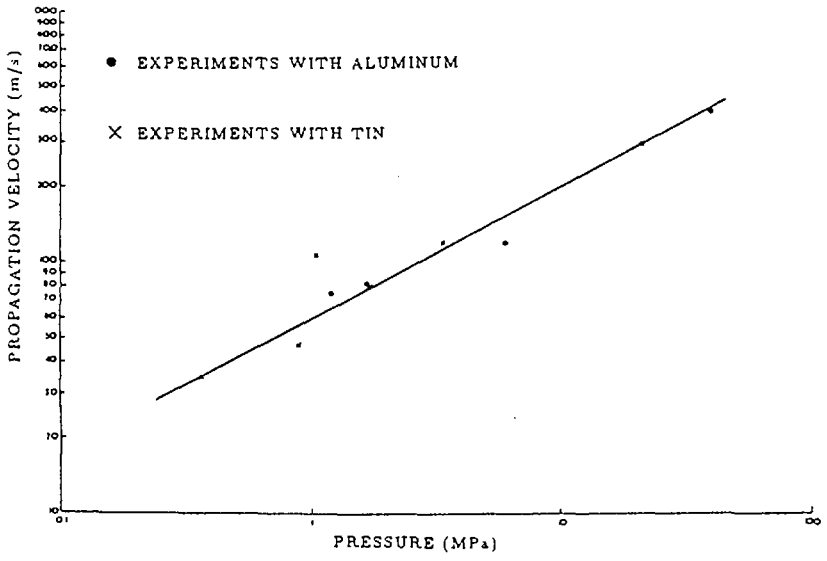

Fig 2. Variation of Propagation Velocity with Peak Pressure, Fry and Robinson

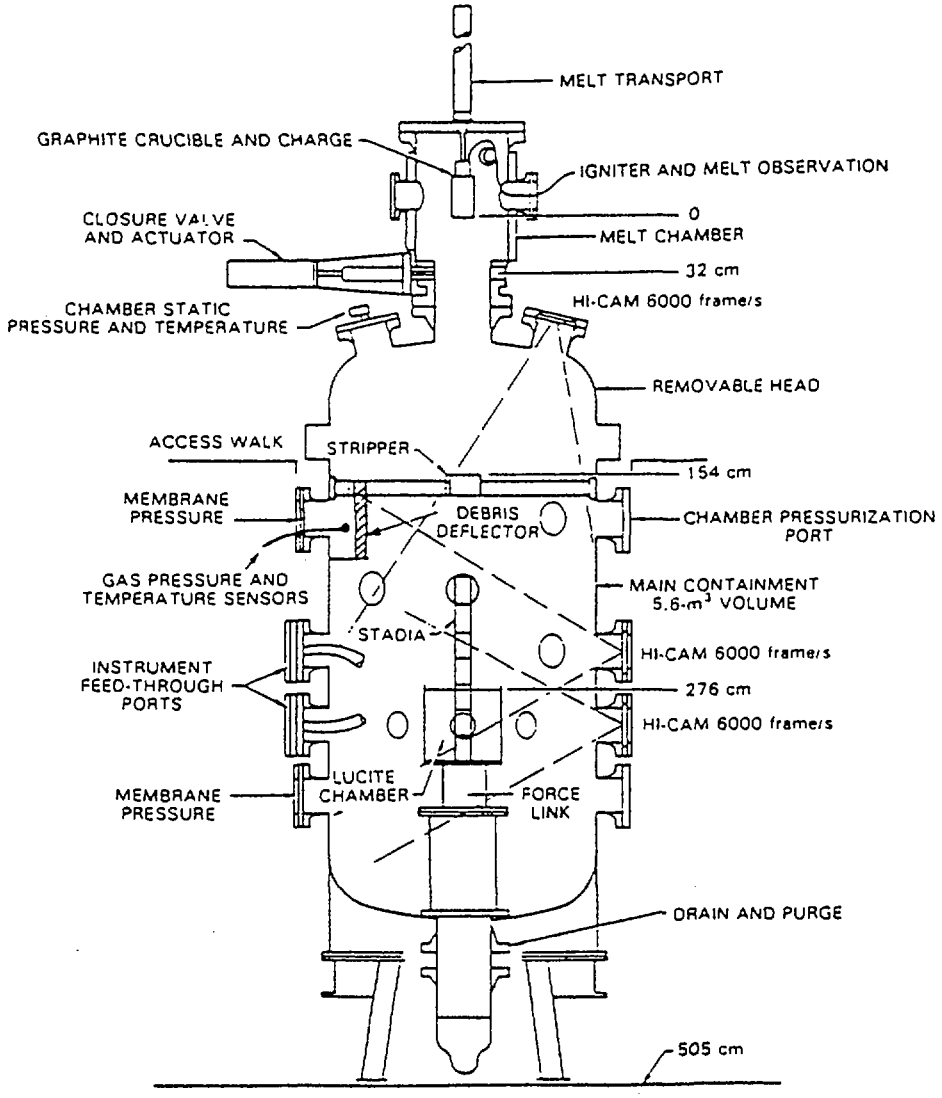

Fig 3. Containment Chamber (Mitchell et al. [29]).

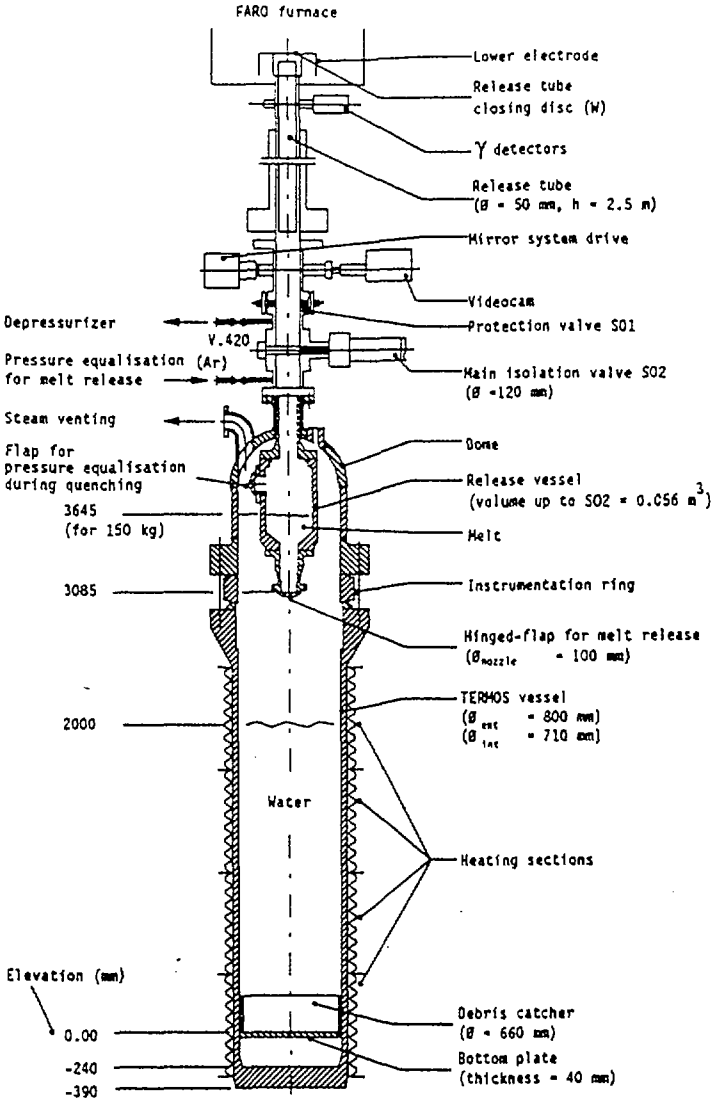

FARO Test Arrangement.

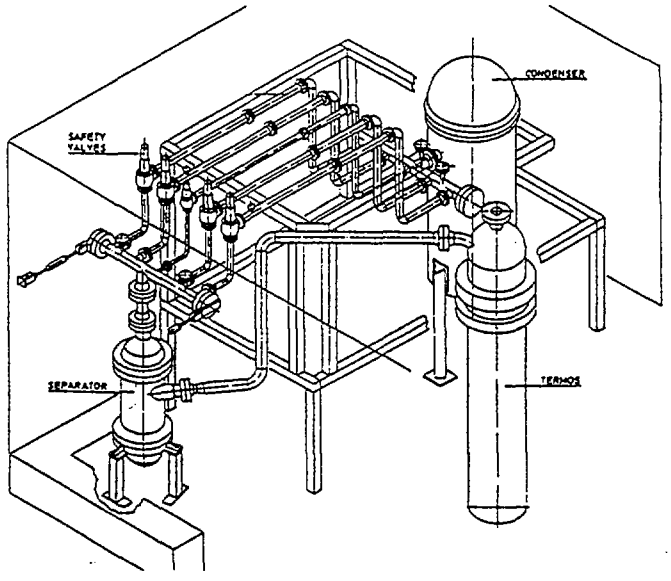

Fig 4. Faro Test Facilities (Test arrangement and venting system)

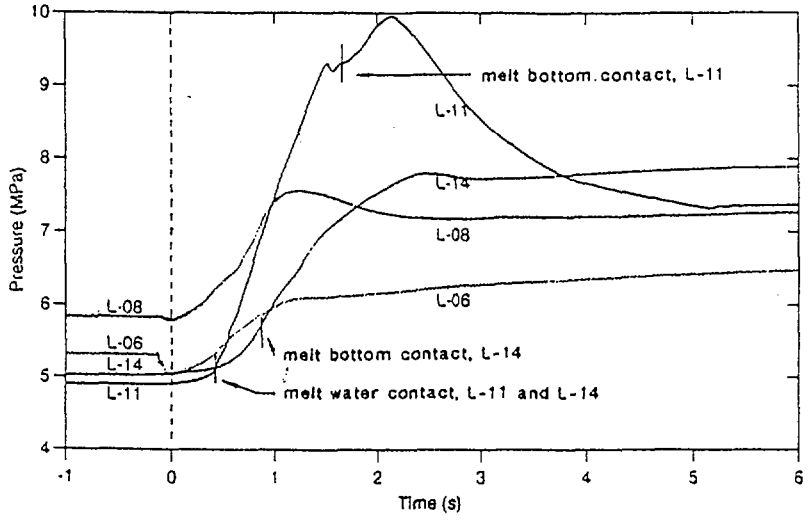

Fig 5. Vessel Pressure History in Test L-06, L-08, L-11, and L-14

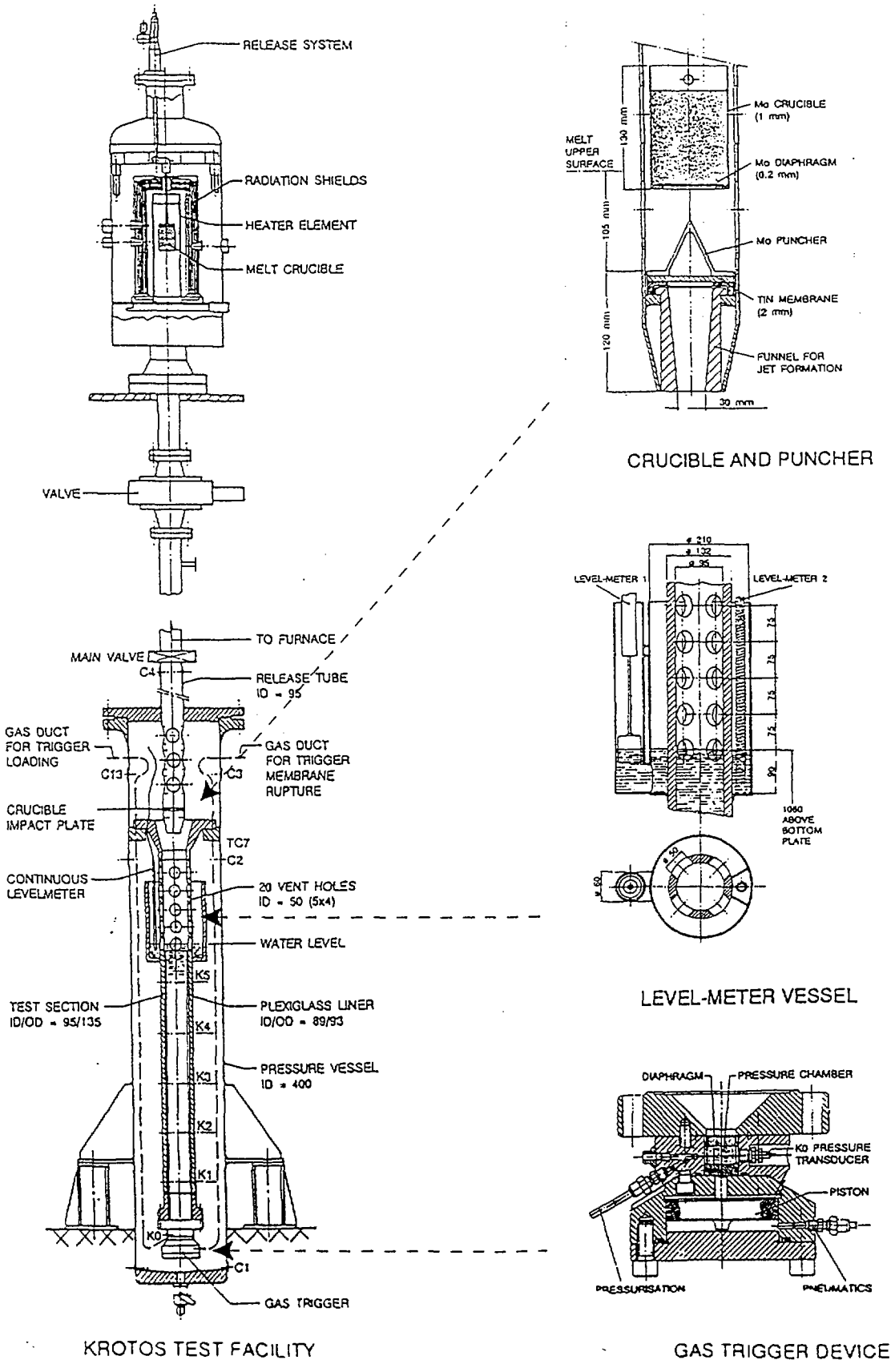

Fig 6. KROTOS Test Facilities

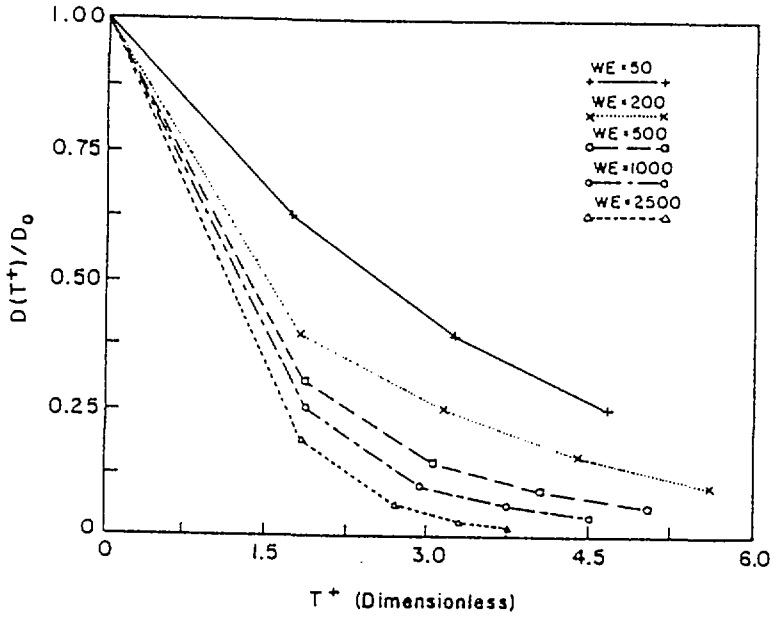

Fig 7. Normalized Fragment Size vs. Dimensionless Time for Different Weber Numbers

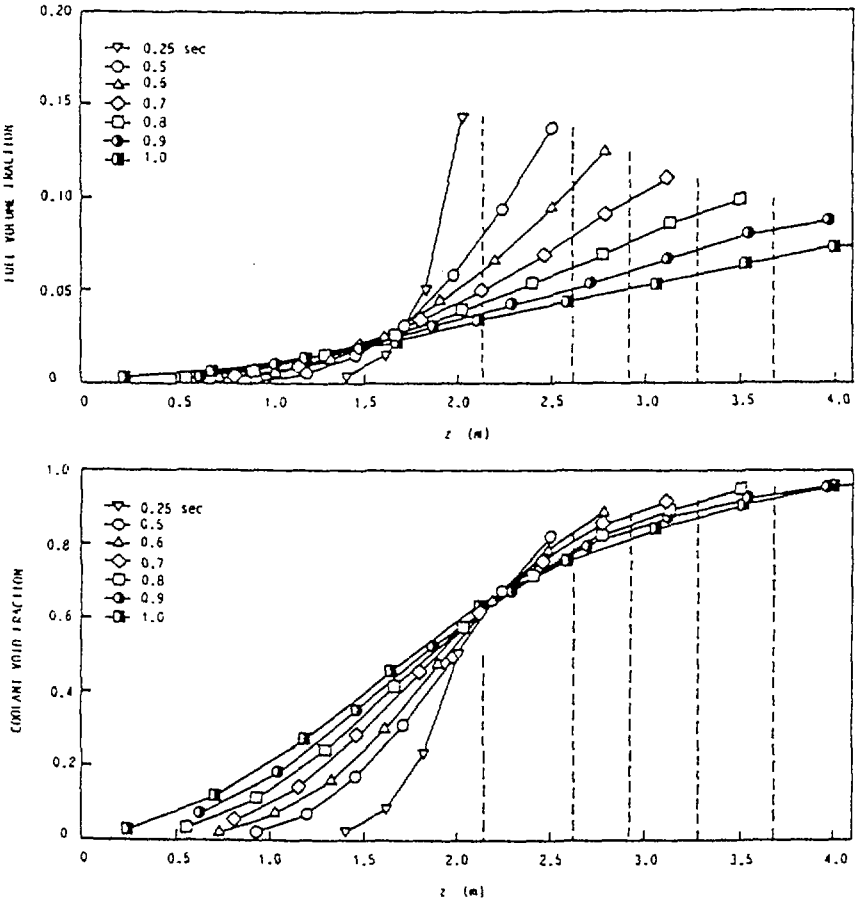

Fig 8. Variation of fuel Volume and coolant void fraction distributions with time during coarse mixing

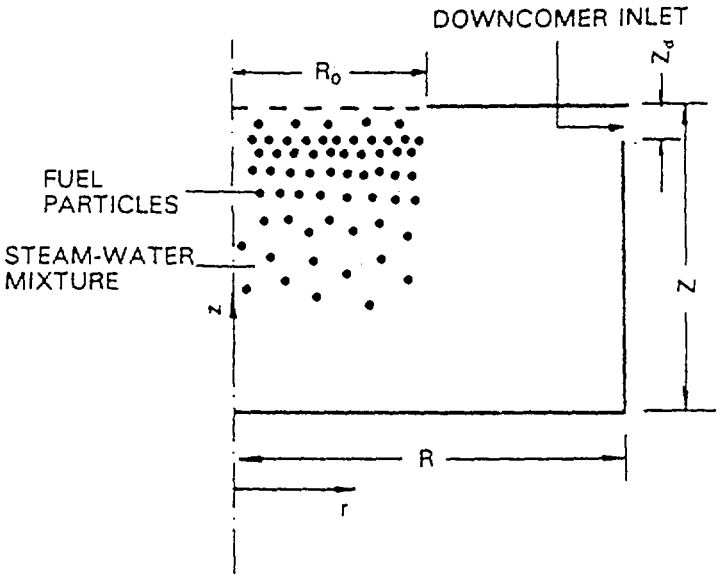

Fig 9. Geometry of Premixing Model, Abolfadl and Theofanous

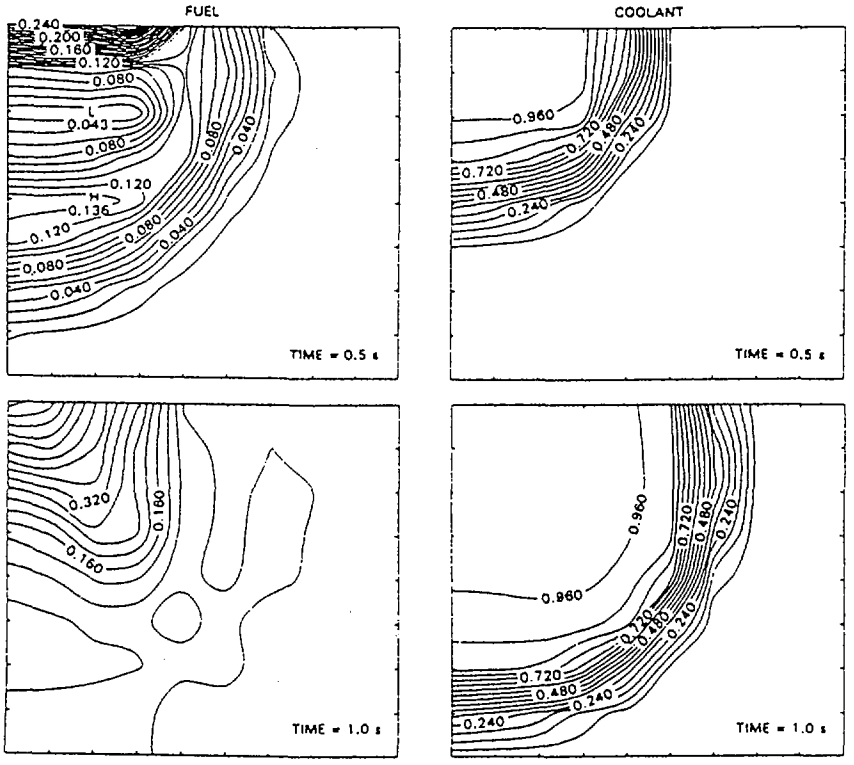

Fig 10. Predicted volume fraction distribution of fuel and coolant at 0.5 and 1.0 second

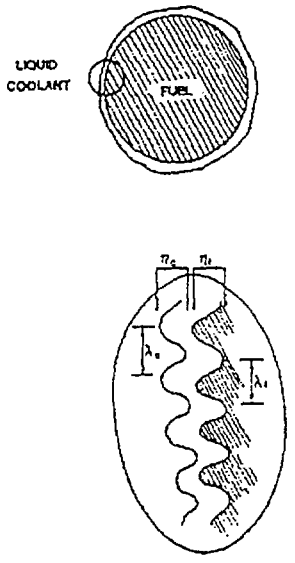

Fig 11. Conceptual Picture of Fuel and Coolant Showing Taylor Instabilities in the Region of Film Collapse

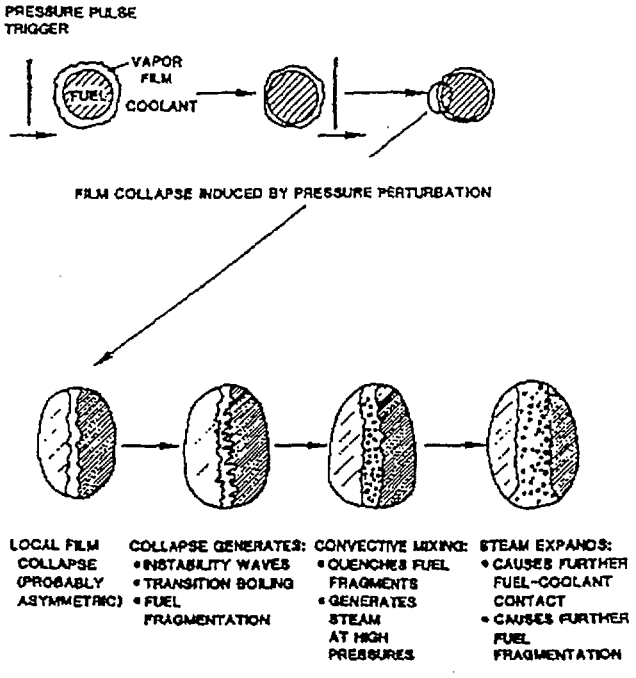

Fig 12. Physical Picture of Thermally Induced Fuel Fragmentation by Taylor Instability

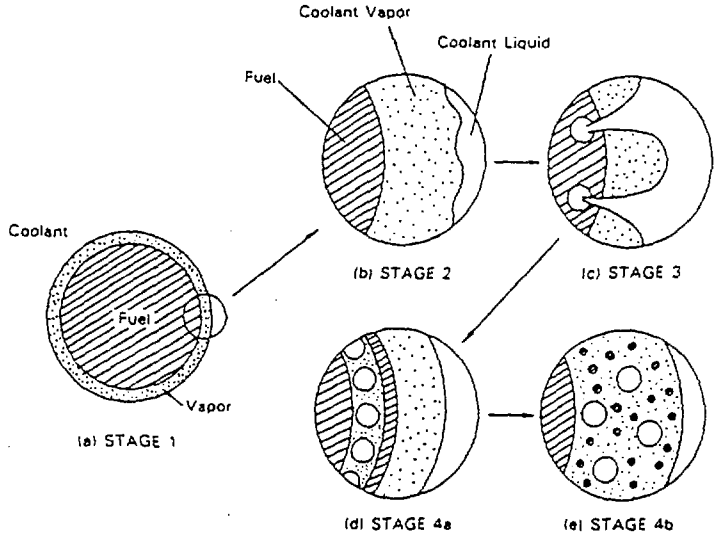

Fig 13. Illustration of Fragmentation by Coolant Entrapment due to Film Collapse and Inward Jet Penetration

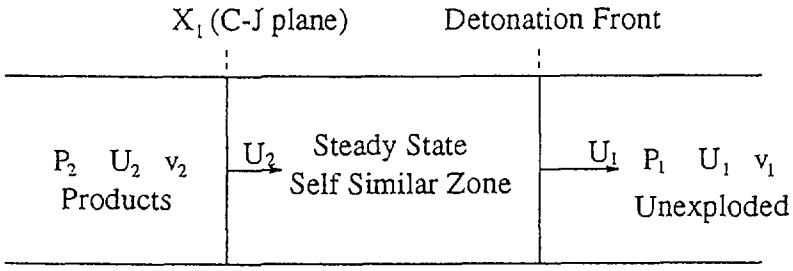

a) Chemical Detonation

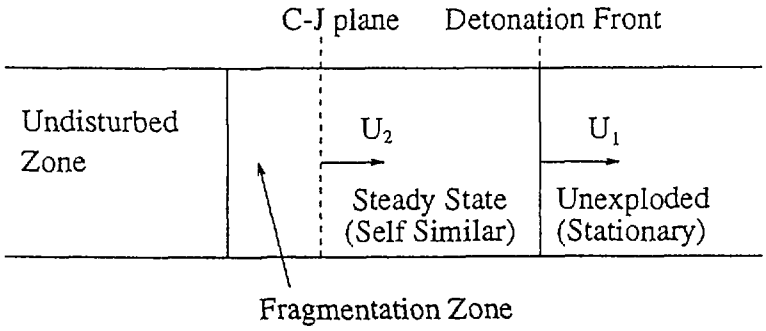

b) Vapor Explosion

Fig 14. Diagram of Steady Detonation Wave viewed from Stationary Frame

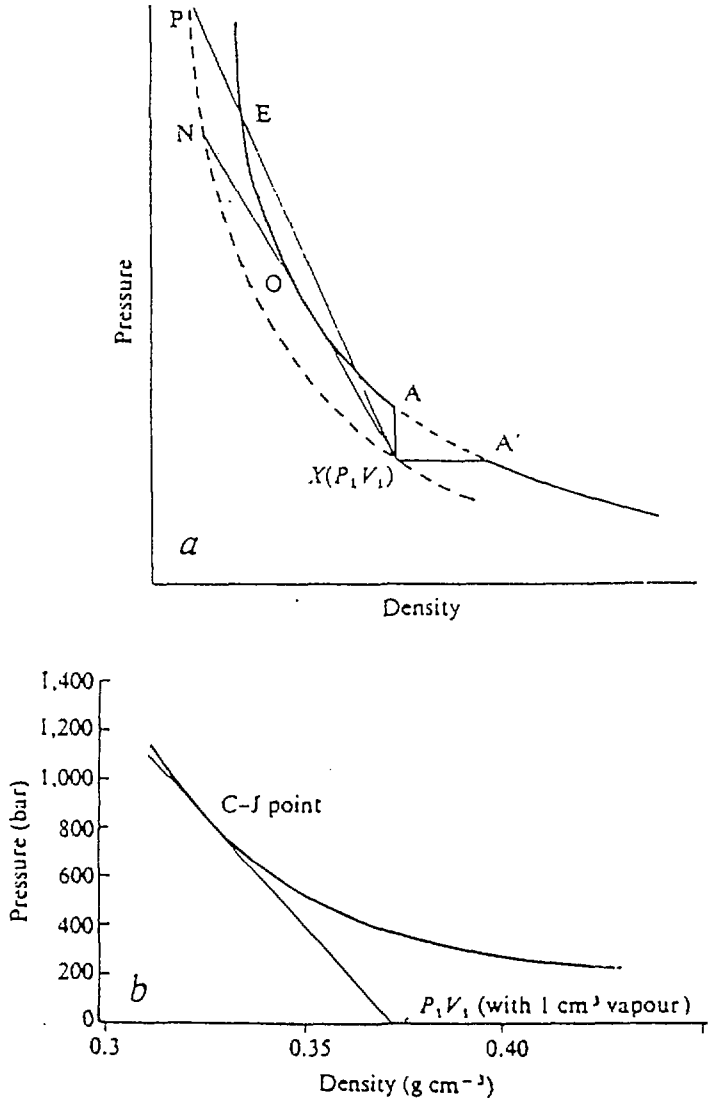

Fig 15. Schematic Shock Adiabatic: Solid Curve for Reacted Material and Dashed Curve for Unreacted Material.

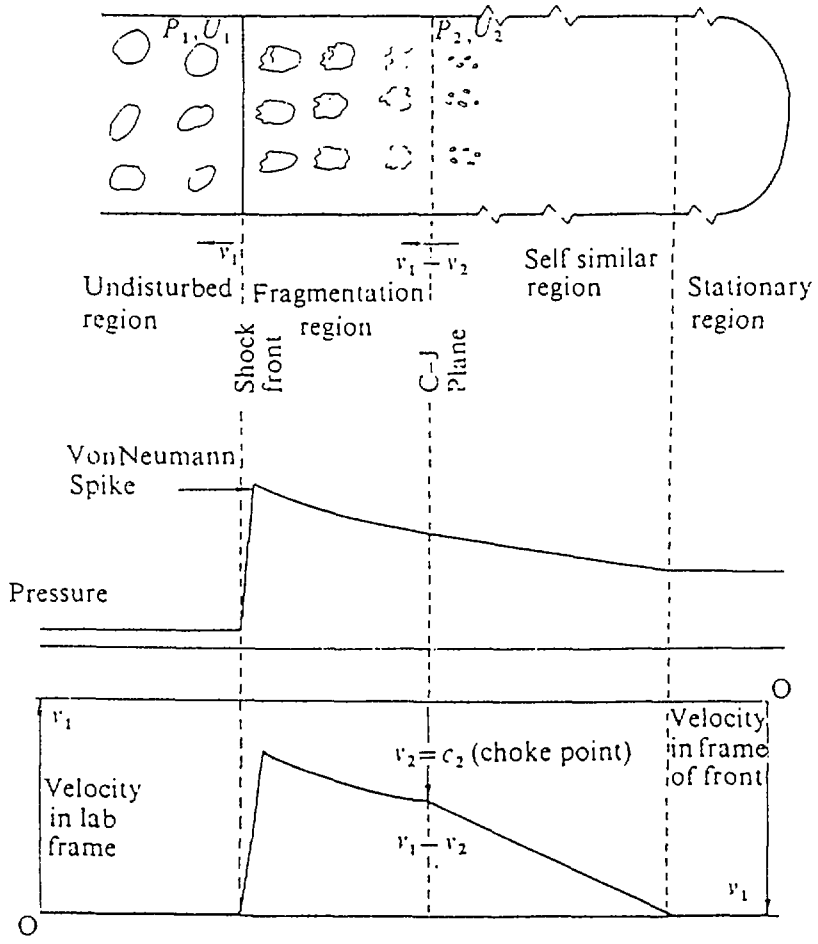

Fig 16. Geometry and Schematic Pressure and Velocity Profiles of a One Dimensional Explosion, Board et al.

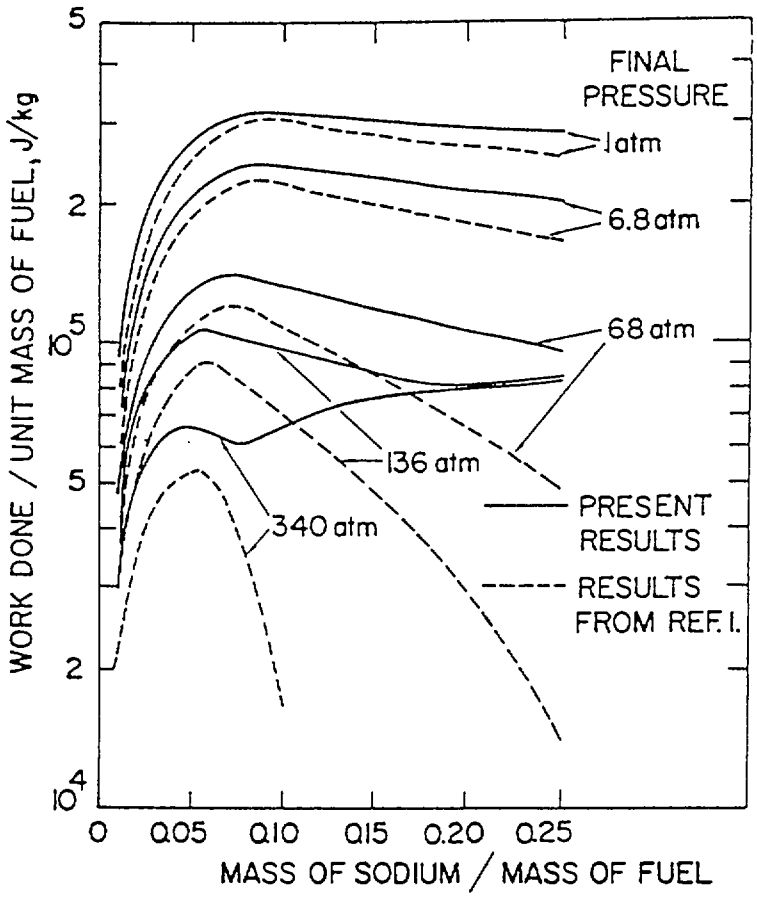

Fig 17. Thermodynamic Work Calculated for UO$_2$ Fuel and Sodium Coolant Compared to Results of Hicks and Menzies

서 지 정 보 양 식			
수행기관보고서번호	위탁기관보고서번호	표준보고서번호	INIS 주제코드
KAERI/AR-534/99			

제목 : 증기폭발 연구현황 보고서

연구 책임자 및 부서명 (TR, AR인 경우 주저자)	황문규(열수력안전연구팀)
연구자 및 부서명	김희동(열수력안전연구팀)

출 판 지	대 전	발행기관	한국원자력연구소	발행년	1999.3
페 이 지	71p	도 표	있음 (v), 없음( )	크기	26 cm
참고사항					

비밀여부	공개(v), 대외비( ) _급비밀 ( )	보고서종류	기술현황 분석보고서(AR)
연구위탁기관		계약번호	

초록(15-20줄 내외)

냉각수가 고온의 용융물과 접할 때 이 용융물의 미세한 분쇄와 이에 따른 냉각수로의 급격한 열전달로 인해 수증기가 폭발적으로 발생할 수 있는데 이 현상을 증기폭발이라 부른다.

증기폭발 현상에서 이에 참여하는 용융물이 많을 경우에는 이로 인한 기계적 에너지의 부하는 상당량에 달해 주변 구조물에 건전성을 위해할 수 있는 충분한 상황이 된다. 따라서 원자로의 노심용융물 동반한 중대사고 시 고온의 노심 용융물은 냉각수와의 접촉으로 증기폭발을 일으킬 수 있게 되고, 이 현상으로 인해 궁극적으로 격납건물의 건전성을 상실할 가능성도 있다.

그간 증기폭발현상을 이해하려는 노력으로 상당한 연구가 진행되어 왔다. 본 보고서에는 이 증기폭발 현상에 대한 실험적 그리고 이론적 연구를 정리한다. 실험적 연구의 경우 보통 20g 이하 질량의 용융물을 다루는 소형실험과 1kg 이상을 용융물로 쓰는 중대형 실험을 모두 다룬다. 또, 이론적 연구에 대해서는 열역학적 모델 및 현상의 진행과정도 포함시키는 기계적 모델도 정리한다.

주제명 키워드 (10단어 내외)	증기폭발, FCI, Steam Explosion, Vapor Explosion

Bibliographic Information Sheet					
Performing Org. Report No.	Sponsoring Org. Report No.		Standard Report No.		INIS Subject Code
KAERI/AR-534/99					
Title : Steam Explosion Studies Review					
Project Manager(or main author) and Department	Hwang, Moonkyu (Thermo-hydraulic Safety Analysis Team)				
Researcher and Department	Kim, Hee-Dong (Thermo-hydraulic Safety Analysis Team)				
Publication Place	Taejeon	Publisher	KAERI	Publication Date	1999.3
Page	71p	Fig. & Tab.	Yes (v), No( )	Size	26 cm
Note					
Classified	Open(v), Restricted( ), _Class DOC. ( )		Report Type	State of the Art Report(AR)	
Sponsoring Org.			Contact No.		

Abstract (15-20 lines)

When a cold liquid is brought into contact with a molten material with a temperature significantly higher than the liquid boiling point, an explosive interaction due to sudden fragmentation of the melt and rapid evaporation of the liquid may take place. This phenomenon is referred to as a steam explosion or vapor explosion.

Depending upon the amount of the melt and the liquid involved, the mechanical energy released during a vapor explosion can be large enough to cause serious destruction. In hypothetical severe accidents which involve fuel melt down, subsequent interactions between the molten fuel and coolant may cause steam explosion. This process has been studied by many investigators in an effort to assess the likelihood of containment failure which leads to large scale release of radioactive materials to the environment.

In an effort to understand the phenomenology of steam explosion, extensive studies has been performed so far. This report presents both experimental and analytical studies on steam explosions. As for the experimental studies, both small scale tests which involve usually less than 20g of high temperature melt and medium/large scale tests where more than 1 kg of melt is used are reviewed. For the modelling part of steam explosions, mechanistic modelling as well as thermodynamic modelling is reviewed.

Subject Keyword (About 10 words)

FCI, Steam Explosion, Vapor Explosion